

Cell Penetrant Inhibitors of the KDM4 and KDM5 Families of Histone Lysine Demethylases. 1. 3-Amino-4-pyridine Carboxylate Derivatives

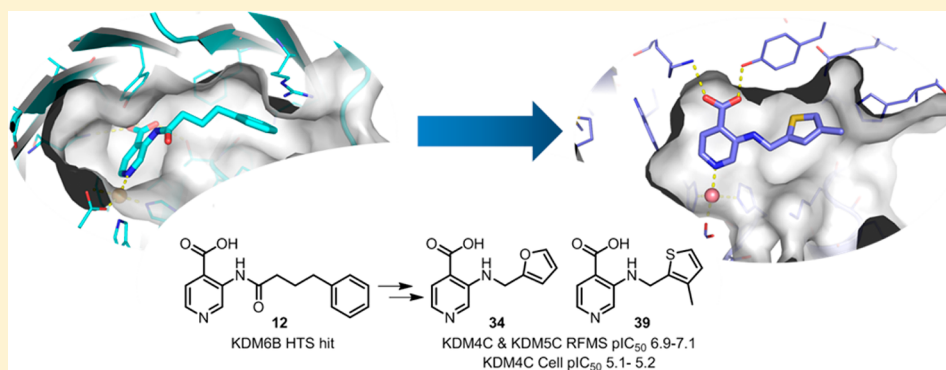
Susan M. Westaway,^{*,†} Alex G. S. Preston,^{*,†} Michael D. Barker,[†] Fiona Brown,[‡] Jack A. Brown,[†] Matthew Campbell,[†] Chun-wa Chung,[‡] Hawa Diallo,[†] Clement Douault,[†] Gerard Drewes,[§] Robert Eagle,[‡] Laurie Gordon,[‡] Carl Haslam,[‡] Thomas G. Hayhow,[†] Philip G. Humphreys,[†] Gerard Joberty,[§] Roy Katso,[‡] Laurens Kruidenier,^{†,#} Melanie Leveridge,[‡] John Little,[†] Julie Mosley,[‡] Marcel Muelbaier,[§] Rebecca Randle,[‡] Inma Rioja,[†] Anne Rueger,[§] Gail A. Seal,[†] Robert J. Sheppard,^{†,||} Onkar Singh,[‡] Joanna Taylor,[‡] Pamela Thomas,[‡] Douglas Thomson,[§] David M. Wilson,^{†,||} Kevin Lee,^{†,⊥} and Rab K. Prinjha[†]

[†]Epinova Discovery Performance Unit, Medicines Research Centre, GlaxoSmithKline R&D, Stevenage SG1 2NY, U.K.

[‡]Platform Technology and Science, Medicines Research Centre, GlaxoSmithKline R&D, Stevenage SG1 2NY, U.K.

[§]Cellzome GmbH, a GSK Company, Meyerhofstrasse 1, 69117 Heidelberg, Germany

S Supporting Information



ABSTRACT: Optimization of KDM6B (JMJD3) HTS hit **12** led to the identification of 3-((furan-2-ylmethyl)amino)pyridine-4-carboxylic acid **34** and 3-(((3-methylthiophen-2-yl)methyl)amino)pyridine-4-carboxylic acid **39** that are inhibitors of the KDM4 (JMJD2) family of histone lysine demethylases. Compounds **34** and **39** possess activity, $IC_{50} \leq 100$ nM, in KDM4 family biochemical (RFMS) assays with ≥ 50 -fold selectivity against KDM6B and activity in a mechanistic KDM4C cell imaging assay ($IC_{50} = 6-8 \mu M$). Compounds **34** and **39** are also potent inhibitors of KDM5C (JARID1C) (RFMS $IC_{50} = 100-125$ nM).

■ INTRODUCTION

Epigenetic post-translation modifications of the N- and C-terminal tails of the histone proteins that form the core of nucleosomes, the basic units of DNA packaging in eukaryotic cell nuclei, play a vital role in the regulation of gene transcription in both healthy and disease states.¹⁻⁴ One of these modifications is methylation of the side chain amino group (N^ϵ) of lysine residues contained within the histone tails. This is a dynamic process controlled by a range of histone lysine methyl transferases (KMTs)^{4,5} and histone lysine demethylases (KDMs)^{4,6} that act in a site specific manner to add and remove up to three methyl groups to and from each lysine. Methylation of specific histone lysine residues may be associated with the formation of euchromatin that is transcriptionally active or poised for activation, e.g., the histone-3-lysine-4 trimethyl (H3K4Me₃) mark. Alternatively, the H3K9Me₃ and H3K27Me₃ marks are strongly associated with heterochromatin

that leads to gene repression.⁴ The Jumonji C (JMJC) family of KDMs consists of iron and 2-oxoglutarate (2-OG) dependent dioxygenases that demethylate N^ϵ -methylated lysine residues present in histone tails. This is thought to proceed through methyl hydroxylation followed by hydrolysis of the intermediate hemiaminal, then loss of formaldehyde.^{4,6} Our interest in understanding how inhibition of members of the KDM4 (also known as JMJD2) family of H3K9Me₃ demethylases affects a range of potentially disease relevant phenotypes led us to undertake a research program aimed at the discovery and development of inhibitors of this family.

A selection of reported inhibitors of the KDM4 family is shown in Figure 1. Many of these have been shown to be

Special Issue: Epigenetics

Received: October 1, 2015

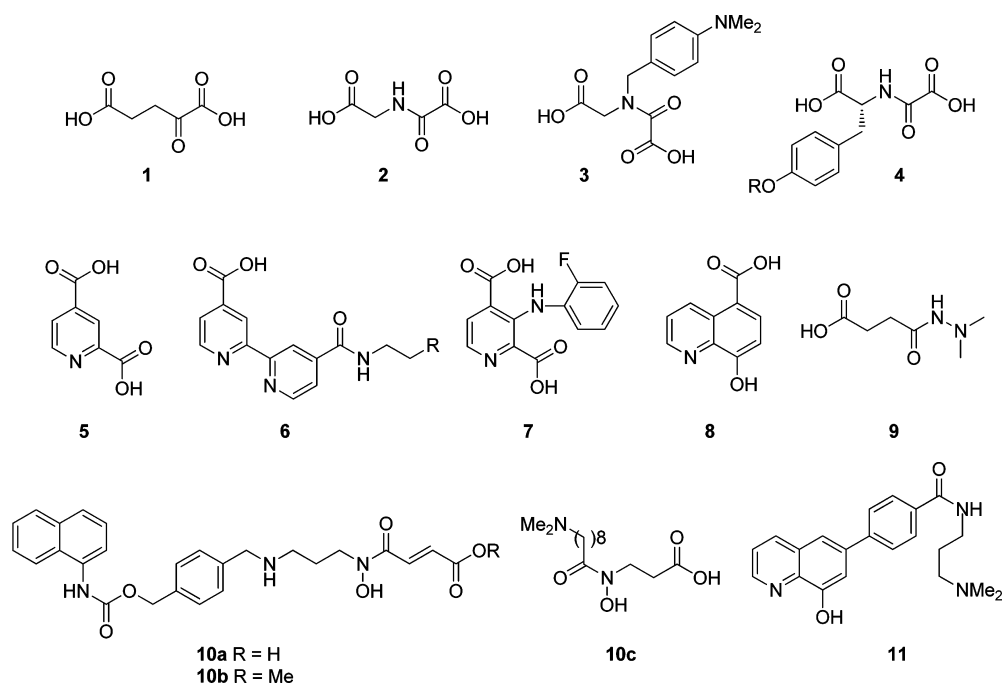


Figure 1. Examples of published compounds with KDM4 (JMJD2) family inhibitory activity.

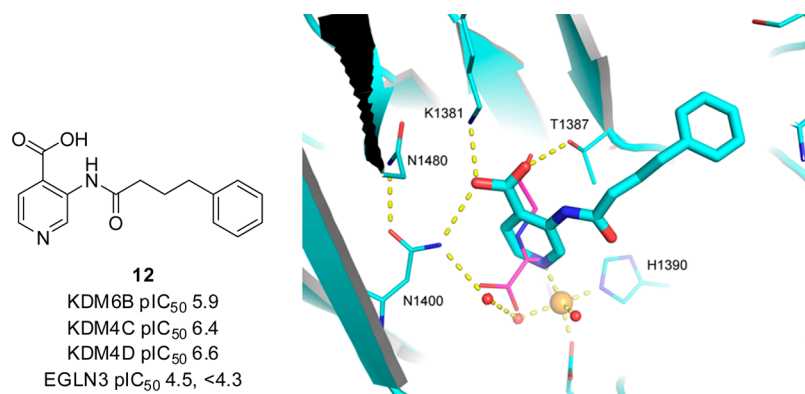


Figure 2. Structure and biochemical screening data for HTS hit **12**: X-ray crystal structure of **12** (cyan, PDB code SFP3) bound to KDM6B with the structure of NOG, **2** overlaid (magenta, from an X-ray structure in KDM6B¹⁹).

competitive with the natural cofactor 2-OG **1**, and one of the earliest inhibitors *N*-oxalylglycine (NOG), **2**,⁷ is a catalytically inert analogue of **1**. Inhibitors such as **3**⁸ and **4**⁹ are elaborated analogues of **2**, and the pyridine carboxylates **5**–**7**^{10–12} maintain at least one of the carboxylate groups present in **2**.

Binding of the 5-carboxy-8-hydroxyquinoline **8**¹³ results in a shift in the active site iron atom when compared with **1**, while the acylhydrazide **9**¹⁴ demonstrates a novel binding mode whereby the compound interacts with the iron through both the carbonyl and terminal dialkylamino moieties. Furthermore, inhibitors that combine 2-OG competitive elements with motifs that are proposed to interfere with peptide substrate binding have also been described, e.g., **10a**¹⁵ and **10c**,¹⁶ as well as sulfur and selenium based inhibitors that act through extrusion of a structural zinc atom present in many members of the KDM4 family.¹⁷ Inhibitors that contain carboxylate moieties generally rely on an ester prodrug approach to enable cellular penetration, and levels of cell activity are typically modest; **10b** (MethylStat), the ester prodrug of pan-KDM inhibitor **10a**, is one of the most potent of this type with reported cellular

activity at $IC_{50} < 10 \mu M$.¹⁴ Non-carboxylate containing 8-hydroxyquinoline, ML324, **11**, has been reported as a chemical probe with submicromolar biochemical activity and promising antiviral cellular activity in the micromolar range.¹⁸

At GSK we initiated a program to discover and develop inhibitors of the KDM4 family with a combination of biochemical activity and physicochemical properties that would lead to cellular activity, ideally in the submicromolar range to enable exploration of phenotypic effects resulting from inhibition of the KDM4 family. In this report we describe the discovery and optimization of a series of 3-aminopyridine-4-carboxylate based inhibitors that led to the identification of cell penetrant analogues with single digit micromolar activity in a KDM4C cellular mechanistic assay.

RESULTS AND DISCUSSION

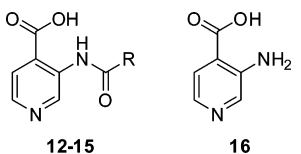
A high throughput screen of the GlaxoSmithKline screening collection against KDM6B (JMJD3) was undertaken as part of our efforts toward the discovery of novel inhibitors of this demethylase, and from this we identified compound **12** as a hit

(Figure 2). In our routine KDM6B SAR assay that utilized the RapidFire mass spectrometry (RFMS) platform,¹⁹ this compound was shown to possess micromolar activity ($pIC_{50} = 5.9$) for its inhibition of demethylation of an H3_(20–36)K27Me₃ peptide analogue by a truncated construct of KDM6B. We also found through cross-screening against KDM4C and KDM4D in equivalent assays utilizing an H3K9Me₃ peptide²⁰ that **12** possessed 3- to 5-fold higher activity at these targets (Figure 2). An homogeneous time-resolved fluorescence (HTRF) assay format was used to assess inhibitory activity against the more distantly related 2-OG utilizing dioxygenase enzyme, the prolyl hydroxylase EGLN3 (also known as PHD3).²¹ In this assay **12** was less potent than in the KDM6B assay with $pIC_{50} \leq 4.5$. Compound **12** contains the pyridine-4-carboxylate core also found in previously disclosed compounds **5** and **7** but lacks the second carboxylate group in the 2-position, thus making it a potentially more attractive starting point for lead optimization targeting cellular penetrant molecules than these dicarboxylates. We therefore initiated a program to explore the SAR of this hit for inhibition of KDM6B and the KDM4 family of histone lysine demethylases.

An X-ray crystallography structure of **12** bound into KDM6B revealed that the pyridine nitrogen formed a key interaction with the metal atom in the active site. The 4-carboxylate group forms a network of interactions with K1381, T1387, and N1400 at the back of the cofactor binding pocket, in a manner similar to that observed for **2** (Figure 2). These interactions of the pyridine carboxylate core of **12** are also similar to those observed for compounds **5** and **6** bound to KDM4A.^{10,11}

Initially, the effects of changing the length of the linker between the pyridine carboxylate core and the terminal phenyl ring were investigated (Table 1). Compounds **12–15** were

Table 1. pIC_{50} Values for **12–16** vs Selected KDM Enzymes and EGLN3²²



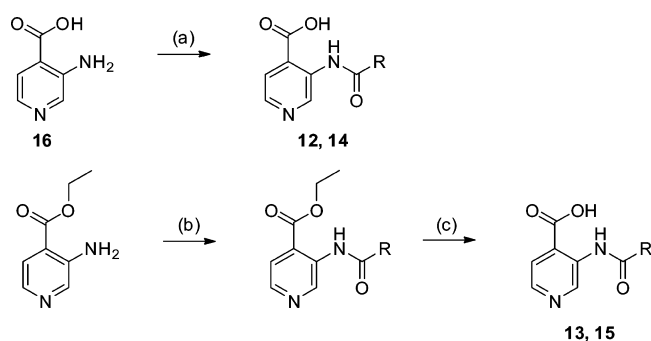
compd	R	KDM6B pIC_{50}	KDM4C pIC_{50}	KDM4D pIC_{50}	EGLN3 pIC_{50}
12	-(CH ₂) ₃ Ph	5.9	6.4	6.6	4.5, <4.3
13	-(CH ₂) ₂ Ph	4.4	6.5	6.4	4.5
14	-CH ₂ Ph	5.4	6.5	6.7	<4.3
15	-Ph	<4.0	5.9	5.8	<4.3
16		4.2 ^a	6.2	5.8	<4.3

^a4.2, $n = 12$; <4.0, $n = 12$.

prepared from either 3-amino-4-pyridinecarboxylic acid **16** or the corresponding ethyl ester and the appropriate acyl chloride using standard amide coupling conditions, followed by ester hydrolysis as required (Scheme 1). Interestingly, reduction of the alkylene linker length from three to two atoms, compound **13** resulted in a significant drop in potency for KDM6B but not for KDM4C and KDM4D. The benzyl analogue **14** showed increased activity at KDM6B when compared with **13**, whereas the phenyl analogue **15** was at least 60-fold selective for KDM4C and KDM4D over KDM6B.

The X-ray crystal structure of **12** bound to KDM6B (Figure 3) showed the phenylpropyl moiety bound in an extended

Scheme 1. Synthesis of 3-Amido-4-pyridinecarboxylic Acids **12–15**^a



^aConditions: (a) RCOCl, ^tPr₂NEt, pyr, DMF, rt, 3.5 d or RCOCl, DMF, 0 °C to rt, 1 h; (b) RCOCl, K₂CO₃, DCM/H₂O, rt, 16 h; (c) LiOH·H₂O, THF/H₂O, rt, 2 h.

conformation with good complementarity to a pocket formed by two β strands lying at the entrance to the active site. The variation in affinity with alkyl chain length may be explained by the position in which the terminal phenyl ring can be placed. For odd numbers of carbons in the chain, **12** and **14**, the phenyl ring can be placed in shape-complementary parts of the pocket. For even numbers or no carbons **13** and **15**, the phenyl would be directed toward the wall of the pocket (toward P1388 and T1330, respectively) and therefore require a strained conformation in order to bind. In KDM4D this pocket has a different shape and the phenyl group in **12** is not bound within the pocket but is directed toward the surface of the enzyme (Figure 3) and therefore the same pattern of variation for the SAR of these compounds is not observed.

We also profiled the fragment core of this series of molecules, 3-amino-4-pyridinecarboxylic acid **16**, and were very interested to find that it represented a highly ligand efficient fragment that was selective for the KDM4 family over KDM6B and EGLN3 (Table 1). The low level of activity of this fragment in our KDM6B assay adds to the SAR evidence described above in which an appropriately positioned side chain is required for good potency at this target. Given the encouraging profile of the phenyl analogue **15**, we continued to investigate the potential for this template to provide selective KDM4 family inhibitors. From this point, the data from the KDM4C RFMS assay only will be reported for most compounds, as this is representative of the levels of inhibitory activity/SAR observed against other KDM4 family members. However, the full profiles against KDM4A, KDM4C, KDM4D, and KDM4E will be detailed for key compounds.

A series of amine analogues **17–25** was also prepared from ethyl-3-amino-4-pyridine carboxylate or 3-amino-4-pyridinecarboxylic acid via reductive amination with the appropriate aldehyde or via nucleophilic substitution of 3-fluoropyridinecarboxylic acid by the appropriate primary amine as shown in Scheme 2.

Removal of the carbonyl oxygen from **15** to afford the benzylamine analogue **17** gave enhanced potency at KDM4C and KDM6B but preserved the 60-fold selectivity for the former (Table 2). The linker length as well as replacement of the terminal aromatic group was therefore investigated in this series. Increasing the length of the alkylene chain, **18–20** resulted in small decreases in KDM4C activity and increases in KDM6B activity. The terminal aromatic group could be replaced with alkyl groups **21–23** to give compounds with

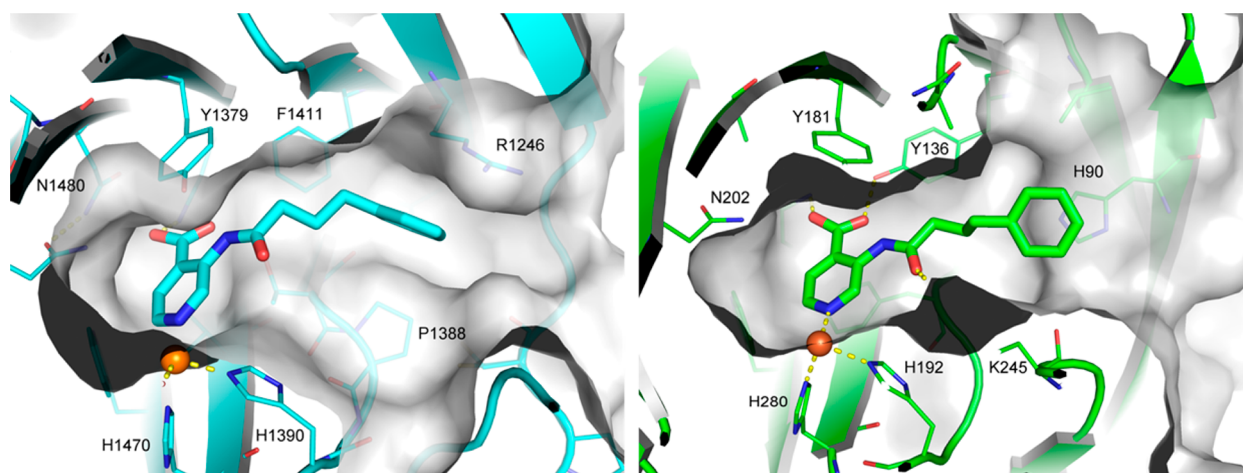


Figure 3. X-ray crystal structures of HTS hit **12** bound to KDM6B (cyan, PDB code 5FP3) and KDM4D (green, PDB code 5FP4).

Scheme 2. General Methods for Synthesis of 3-Aminopyridinecarboxylic Acids 17–43

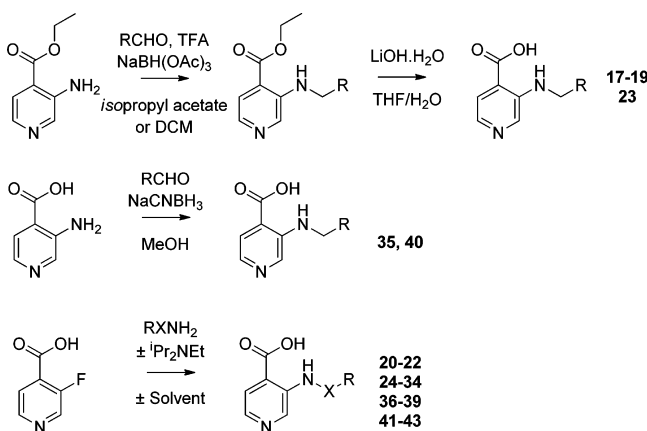


Table 2. Activity of Benzylamine Derivatives 17–25 vs KDM4C and KDM6B²²

compd	R	KDM4C RFMS pIC ₅₀	KDM6B RFMS pIC ₅₀
17	-Ph	7.0	5.2 ^a
18	-CH ₂ Ph	6.4	5.6
19	-(CH ₂) ₂ Ph	6.7	6.1
20	-(CH ₂) ₃ Ph	6.8	6.2
21	-CH ₂ CH ₃	6.5	5.4
22	-(CH ₂) ₂ CH ₃	6.9	5.6
23	-CH(CH ₃) ₂	6.8	5.7
24	-CH ₂ NH ₂	4.2	<4.0
25	-(CH ₂) ₂ NH ₂	6.3	<4.0

^a5.2, *n* = 8; <4.0, *n* = 1.

IC₅₀ less than 1 μM at KDM4C but with only a 13- to 20-fold selectivity window over KDM6B.

Interestingly, the introduction of a polar group in the form of a terminal primary amine resulted in low, unmeasurable activity at KDM6B, but the activity at KDM4C depended on the length of the alkylene linker. The ethylene linked side chain **24** was not well tolerated, whereas the propylene linked analogue **25**

possessed submicromolar KDM4C activity. However, this potency was still lower than that of propyl analogue **22**, indicating that the amino group is not forming an energetically productive interaction with the protein. For all of these compounds, activity against EGLN3 (PHD3) had been reduced to below detectable levels (pIC₅₀ < 4.3).

Given the interesting overall profile of **17**, we further profiled the compound against other members of the KDM4 family as shown in Table 3. Compound **17** showed high levels of biochemical activity at KDM4A, KDM4D, and KDM4E in addition to KDM4C.

Table 3. Inhibition Profile of **17** vs KDM4 Family Members in RFMS Assays²²

compd	KDM4A pIC ₅₀	KDM4C pIC ₅₀	KDM4D pIC ₅₀	KDM4E pIC ₅₀
17	6.9	7.0	7.2	7.4

A crystal structure of **17** bound to KDM4D shows the pyridine carboxylate core of this series anchors compounds in a conserved manner within the 2-OG site (Figure 4a). The flexible linker of **17** allows the terminal phenyl to lie against a pocket flanked by hydrophobic residues such as Y136, A138 on one side, while a water mediated interaction between D139 and K245 closes off another edge.

To evaluate cellular activity, we utilized a mechanistic, high content imaging assay: U2OS cells were subjected to a Bacmam-mediated transfection with full-length HALO-tagged KDM4C in the presence of test compound, incubated at 37 °C for 24 h, then fixed and stained.

Those cells that expressed the Halo-tagged KDM4C in the nuclear region above a threshold level were analyzed to determine the level of global H3K9Me₃ demethylation. A signal window for demethylation was established using DMSO as a negative vehicle control and the iron chelator desferrioxamine (DFO) as a positive control. On testing in this assay, compound **17** demonstrated a modest potency, pIC₅₀ = 4.4 (IC₅₀ = 40 μM), which was some 400-fold lower than its biochemical potency and too low for use as a probe molecule for exploration of potential phenotypic responses associated with KDM4 family inhibition.

We also assessed a prodrug approach analogous to that successfully used for our previously described pyridylpyrimidine inhibitors of the KDM6 family (JMJD3/UTX).¹⁹ Compound

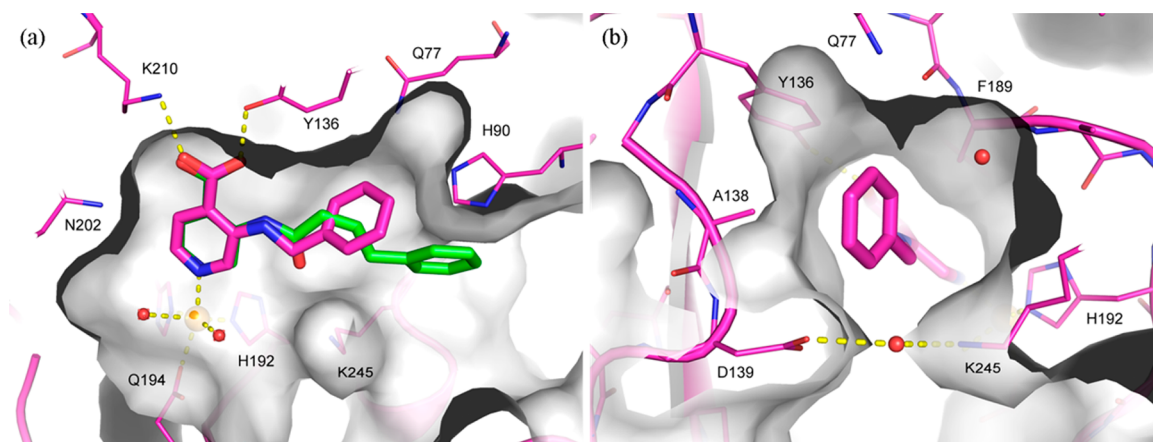
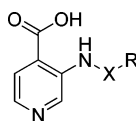


Figure 4. X-ray crystal structure of **17** (magenta stick format, PDB code 5FP7) bound to KDM4D (magenta lines, white surface). (a) Overlaid with **12** (green; PDB code 5FP4). (b) Phenyl ring of **17** sits in a pocket created by a water bridged interaction between K245 and D139 lined on one side by hydrophobic residues of A138 and Y136.

Table 4. Biochemical and Cellular Activity of Benzylamine Derivatives **17–43** vs KDM4C²²



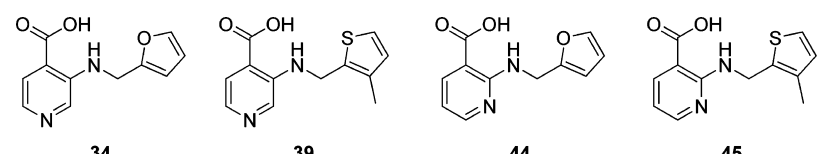
compd	X	R	KDM4C RFMS pIC ₅₀	KDM4C cell pIC ₅₀	ΔpIC ₅₀ (RFMS-cell)	cLogP	ChromLogD _{pH7.4}
17	CH ₂	Ph	7.0	4.4	2.6	3.4	0.7
26	CH ₂	2,5-Me ₂ Ph	6.2	4.3 ^a	1.9	4.4	1.7
27	CH ₂	2,3-Me ₂ Ph	6.5 ^b	4.8	1.7	4.3	1.7
28	CH ₂	3-biphenyl	5.7	<4.0	>1.7	5.3	2.2
18	CH ₂	CH ₂ Ph	6.4	4.5 ^c	1.9	4.1	1.3
20	CH ₂	(CH ₂) ₃ Ph	6.8	5.2	1.6	5.0	2.0
29	CH ₂	<i>c</i> -hexyl	6.9	5.3	1.6	4.6	1.7
30	CH ₂	<i>c</i> -pentyl	6.7	5.2	1.5	4.1	1.3
31	CH ₂	<i>c</i> -propyl	6.9	4.5	2.4	2.9	0.1
32	CH ₂	2-thienyl	7.2	5.2	2.0	3.1	0.5
33	CH ₂	3-thienyl	7.2	5.2	2.0	3.1	0.6
34	CH ₂	2-furyl	7.1	5.1	2.0	2.6	0.1
35	CH ₂	4-thiazolyl	7.0	4.5	2.5	1.8	-0.5
36	CH ₂	5-pyrazolyl	6.9	<4.0	>2.9	1.5	-0.7
37	CH ₂	5-Me-2-thienyl	6.7	4.7	2.0	3.6	1.1
38	CH ₂	4-Me-2-thienyl	7.0	5.1	1.9	3.6	1.2
39	CH ₂	3-Me-2-thienyl	7.1	5.2	1.9	3.5	1.1
40	CH ₂	2-benzothienyl	5.9	4.4	1.5	4.4	1.8
41	CHMe	Ph	6.2	4.2	2.0	3.7	1.2
42	CMe ₂	Ph	5.8	nd		4.1	1.4
43	CHPh	Ph	5.2	nd		4.8	2.3

^a4.3, *n* = 1; <4.0, *n* = 1. ^b6.5, *n* = 3; <4.0, *n* = 1. ^c4.5, *n* = 6; <4.0, *n* = 2.

20 possessed submicromolar biochemical potency at KDM6B, but when its ethyl ester (**20E**) (Supporting Information Figure 1) was tested for its ability to inhibit TNF production by LPS-stimulated human primary macrophages, no inhibition was observed (data not shown). It is possible that the lack of cellular activity of putative prodrug **20E** is a result of less efficient hydrolysis of this more hindered ester in the cell, or potentially reduced cellular penetration, although **20E** is more lipophilic (cLogP = 5.4) than the previously described KDM6 family prodrug ethyl 3-((6-(4,5-dihydro-1*H*-benzo[*d*]azepin-3(2*H*)-yl)-2-(pyridin-2-yl)pyrimidin-4-yl)amino)propanoate (GSK-J4)¹⁹ (cLogP = 4.8). This result, combined with a desire not to restrict the potential utility of these inhibitors to

phenotypic investigations in esterase-containing cell types, led us to prepare a range of analogues (**26–43**, Scheme 2) of lead benzylamine compound **17** with the aim of determining if improved cellular potency could be achieved through further modulation of biochemical activity and physicochemical properties.

From the data presented in Table 4 it can be seen that KDM4C RFMS potency of less than 100 nM (pIC₅₀ ≥ 7.0) could be achieved with a number of five-membered heteroaryl replacements of the terminal phenyl group (**32–35**, **38**, **39**). From the examples explored, replacement of the phenyl group with cycloalkyls **29–31** was not detrimental to potency at KDM4C. When steric constraints were pushed further, a more

Table 5. Further Profiling of Cell Active Monocarboxylic Acid Inhibitors **34** and **39** with Inactive Control Analogues **44** and **45**²²


compd	KDM4A RFMS pIC ₅₀	KDM4C RFMS pIC ₅₀	KDM4D RFMS pIC ₅₀	KDM4E RFMS pIC ₅₀	KDM6B RFMS pIC ₅₀	KDM5C RFMS pIC ₅₀	KDM4C cell pIC ₅₀	KDM5C cell pIC ₅₀
34	7.0	7.1	7.0	7.4	4.9	7.0	5.1	4.2 ^a
39	7.0	7.1	7.0	7.3	5.3	6.9	5.2	4.6
44	<4.0	<4.0	<4.0	<4.0	nt ^b	<4.0	<4.0	<4.0
45	<4.0	<4.0	<4.0	<4.0	<4.0	<4.0	<4.0	<4.0

^a4.2, *n* = 3; <4.0, *n* = 4. ^bnt = not tested.

significant drop in potency occurred; for example, the biphenyl **28** and benzothienyl **40** analogues showed decreases of 12- to 20-fold. Substitution at the benzylic carbon atom also resulted in reduced potency (**41–43**) with the hindered dibenzylidene analogue **43** showing a 60-fold decrease compared to **17**. Taken together these data indicate that the region of the active site that is occupied by this substituent is relatively open to a range of substitution patterns, although bulky substituents in the vicinity of the core appear to be less favored.

Examining the effects of these substituents on cellular activity revealed that there is a significant downward potency shift when moving into a whole cell assay as may be expected for compounds containing a carboxylate moiety. The lipophilicity data for compounds **17–40** are presented in terms of both calculated log *P* (cLog*P*) and measured chromatographic log *D* at pH 7.4 (ChromLog*D*_{pH7.4}).²³ There is a reasonable correlation between the drop in potency from biochemical to cell assay [expressed as Δ*pIC*₅₀ (RFMS-cell)] and cLog*P* or ChromLog*D* with the more lipophilic compounds tending to show a smaller decrease, thus indicating higher cell penetration (Table 4 and Supporting Information Figure 2). Compounds **20**, **27**, **29**, **30**, and **40** showed a 50-fold or lower decrease (Δ*pIC*₅₀ ≤ 1.7) and possessed cLog*P* values higher than 4. A number of these analogues also possessed single digit micromolar potency (pIC₅₀ > 5) in the cell assay (**20**, **29**, **30**). This level of cell activity could also be achieved with compounds that are less lipophilic (cLog*P* = 2.9–3.6) but possess increased biochemical potency, typically pIC₅₀ ≥ 7 (IC₅₀ ≤ 100 nM) (**32–34**, **38**, **39**). The interesting level of cell activity demonstrated by these carboxylic acids led us to further profile exemplars **34** and **39** across the KDM4 family and at KDM6B and KDM5C as shown in Table 5. Compounds **34** and **39** were also tested for their activity against prolyl hydroxylase EGLN3 and found to possess negligible activity (pIC₅₀ ≤ 4.1).

Also included for comparison are compounds **44** and **45** that are the KDM4 family inactive isomers of **34** and **39**, wherein the pyridine nitrogen atom has been translocated relative to the carboxylate. This renders the nitrogen no longer able to interact with the active site iron given the expected binding mode of these molecules within KDM4 enzymes, as was confirmed by crystallography of the 4-methylthienyl analogue **38** within KDM4D (Figure 5).

Interestingly, while compounds **34** and **39** are equipotent across the KDM4 family and selective vs KDM6B and EGLN3, we found that they are potent inhibitors of the H3K4Me_{3/2} demethylase KDM5C (JARID1C). This activity translated into

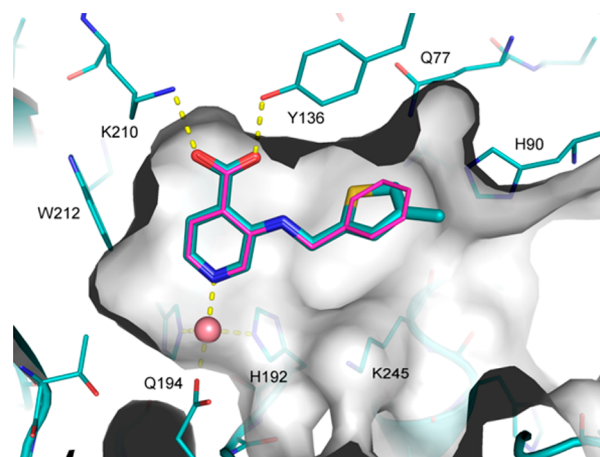


Figure 5. X-ray crystal structure of **38** (blue stick format, PDB code 5FP8) bound to KDM4D (blue lines, white surface) overlaid with **17** (magenta stick, PDB code 5FP7). The conserved binding of the two molecules is apparent, with the 4-methylthiophene of **38** occupying the same space as the phenyl ring of **17**.

the cellular context utilizing a similar mechanistic, high content imaging assay to that described earlier for KDM4C although the levels of activity in the KDM5C cell assay were lower than for KDM4C. The reasons for this reduced cellular activity at KDM5C when compared to KDM4C are not clear. The assay uses the same U20S cells and protocol, but it is plausible that differences in the efficiency of expression of the two targets in the cells and/or differences in the affinity of the two enzymes for the natural cofactor 2-OG, with which these inhibitors compete, may play a part. Compounds **34** and **39** were also profiled in our in-house selectivity panel of nonrelated drug and liability targets. Compound **34** showed measurable activity in 3/48 assays and compound **39** in 5/49 assays (Supporting Information Tables 1 and 2). All potencies were ≥25 μM except for that of compound **39** in the OATP1B1 transporter inhibition assay where it possessed an IC₅₀ value of 8 μM. Compound **34** and KDM4C “inactive” analogues **44** and **45** had no measurable activity in this assay (IC₅₀ > 50 μM).

CONCLUSION

In summary, we have optimized a pyridine monocarboxylate KDM6B HTS hit to a series of potent inhibitors of the KDM4A, KDM4C, KDM4D, KDM4E, and KDM5C histone lysine demethylases.²⁴ Furthermore, exemplars such as **34** and **39** possessed interesting activity in a target specific, cellular

mechanistic assay against overexpressed KDM4C with IC_{50} values of $<10 \mu M$. Activity was also observed against overexpressed KDM5C albeit with lower potency. In the limited set of biochemical assays utilized to assess selectivity during this program of work, compounds **34** and **39** showed low levels of activity vs KDM6B and EGLN3. Further profiling to assess the selectivity of compound **34** against a broader subset of 2-OG dependent dioxygenases, including other KDM enzymes, was undertaken using a chemical proteomics based approach developed in our laboratories, and this will be published in due course.²⁵

These compounds may have utility in exploring the phenotypic effects of KDM4 and KDM5 family inhibition when used in combination with negative control molecules such as **44** and **45**. However, we were keen to explore whether we could maintain or improve on the levels of activity observed in this series with less acidic and thus potentially more cell penetrant compounds, targeting cellular activity with $pIC_{50} \geq 6$ ($IC_{50} \leq 1 \mu M$), and our findings are reported in the accompanying article.²⁶

EXPERIMENTAL SECTION

Chemistry. All commercial chemicals and solvents are reagent grade and were used without further purification unless otherwise specified. Reactions were monitored by thin-layer chromatography on 0.2 mm silica gel plates (POLYGRAM SIL G/UV254, Macherey-Nagel) and were visualized with UV light. Compounds were typically purified by automated flash silica chromatography (Biotage SP4), manual chromatography on prepacked cartridges (SPE), or mass directed autopreparative chromatography (MDAP). Where specifically indicated, the following MDAP methods were used. For the formic method, the HPLC analysis was conducted on a Sunfire C18 column (150 mm \times 30 mm i.d., 5 μm packing diameter) at ambient temperature, eluting with 0.1% formic acid in water and 0.1% formic acid in acetonitrile using an elution gradient. The UV detection was an averaged signal from wavelength of 210 to 350 nm. The mass spectra were recorded on a Waters ZQ mass spectrometer using alternate-scan positive and negative electrospray. Ionization data were rounded to the nearest integer. For the high pH method, the HPLC analysis was conducted on an XBridge C18 column (100 mm \times 30 mm, i.d. 5 μm packing diameter) at ambient temperature, eluting with 10 mM ammonium bicarbonate in water adjusted to pH 10 with ammonia solution, and acetonitrile using an elution gradient. The UV detection was an averaged signal from wavelength of 210 to 350 nm. The mass spectra were recorded on a Waters ZQ mass spectrometer using alternate-scan positive and negative electrospray. Ionization data were rounded to the nearest integer. 1H and ^{13}C NMR spectra were recorded on either a Bruker DPX-400 spectrometer at 400 and 126 MHz, respectively, or a Bruker AV-600 spectrometer at 600 and 150 MHz, respectively. Chemical shifts are reported in parts per million (ppm, δ units). Splitting patterns are designated as s, singlet; d, doublet; t, triplet; q, quartet; m, multiplet; br, broad; etc. LCMS spectra were recorded on an Acquity UPLC BEH C18 column (50 mm \times 2.1 mm i.d., 1.7 μm packing diameter) at 40 °C. The UV detection was a summed signal from wavelength of 210 to 350 nm. The mass spectra were recorded on a Waters ZQ mass spectrometer using alternate-scan positive and negative electrospray. Ionization data were rounded to the nearest integer. As specifically indicated, the compounds were eluted by one of the following LCMS methods. For the formic method, elution was with 0.1% v/v solution of formic acid in water (solvent A) and 0.1% v/v solution of formic acid in acetonitrile (solvent B) using the following elution gradient: 0–1.5 min 3–100% B, 1.5–1.9 min 100% B, 1.9–2.1 min 3% B at a flow rate of 1 mL/min. For the high pH method, elution was with 10 mM ammonium bicarbonate in water adjusted to pH 10 with ammonia solution (solvent A) and acetonitrile (solvent B) using the following elution gradient: 0–1.5 min 1–97% B, 1.5–1.9 min 97% B, 1.9–2.1

min 100% B at a flow rate of 1 mL/min. For the TFA method, elution was with 0.1% v/v solution of trifluoroacetic acid in water (solvent A) and 0.1% v/v solution of trifluoroacetic acid in acetonitrile (solvent B) using the following elution gradient: 0–1.5 min 3–100% B, 1.5–1.9 min 100% B, 1.9–2.0 min 100–3% B at a flow rate of 1 mL/min. High resolution mass spectra (HRMS) were acquired as profile data using a Thermo Scientific LTQ Orbitrap mass spectrometer, equipped with an ESI interface, over a mass range of 120–1000 Da at a mass resolution of 100 000. A commercial calibration solution (Pierce LTQ ESI positive ion calibration solution) was used to externally calibrate the instrument prior to analysis. Ionization was achieved with a spray voltage of 4 kV, a capillary voltage of 45 V, tube lens voltage of 110 V, with sheath and auxiliary gas flows of 40 and 20 (arbitrary units), respectively. The capillary temperature was maintained at 300 °C. The elemental composition was calculated using Xcalibur (version 2.0.7) for the $[M + H]^+$ and the mass error quoted as ppm; an error of <5 ppm indicates that the measured mass is consistent with the proposed formula. Melting point analysis was carried out using a Stuart SMP40 melting point apparatus, and melting points are uncorrected. The purity of all compounds screened in the biological assays was found to be $\geq 95\%$ by LCMS analysis unless otherwise specified.

3-(4-Phenylbutanamido)isonicotinic Acid, 12. To 3-amino-4-pyridinecarboxylic acid (500 mg, 3.62 mmol) in DMF (10 mL) were added *N*-ethyl-*N*-isopropylpropan-2-amine (1264 μL , 7.24 mmol) and pyridine (293 μL , 3.62 mmol). The reaction was stirred, and 4-phenylbutanoyl chloride (596 μL , 3.62 mmol) was added. The reaction mixture was stirred at room temp for 3.5 days. The solid was collected by filtration and washed with EtOAc and MeOH, then dried in vacuo. MeOH (15 mL) was added to the crude, and the resulting solution was filtered and loaded onto an SCX column. The column was washed with MeOH, and the product was eluted using 2 M NH_3 in MeOH. The fractions were concentrated to afford **12** as a white solid (555 mg, 54%). LCMS (TFA method) retention time 0.67 min, $[M + H]^+ = 285$. 1H NMR (600 MHz, DMSO- d_6) δ ppm 1.93 (quin, $J = 7.3$ Hz, 2H), 2.39 (t, $J = 7.5$ Hz, 2H), 2.65 (t, $J = 7.5$ Hz, 2H), 7.18 (t, $J = 7.3$ Hz, 1H), 7.23 (d, $J = 7.0$ Hz, 2H), 7.29 (t, $J = 7.8$ Hz, 2H), 7.76 (d, $J = 4.8$ Hz, 1H), 8.30 (d, $J = 5.1$ Hz, 1H), 9.55 (s, 1H).

3-(2-Phenylacetamido)isonicotinic Acid, 14. Phenylacetyl chloride (0.240 mL, 1.810 mmol) was added dropwise to a stirred suspension of 3-aminonicotinic acid (250 mg, 1.810 mmol) in DMF (5 mL) at 0 °C under N_2 . After stirring at 0 °C for 5 min, the flask was removed from the cooling bath and allowed to stir at rt for 1 h by which time a solution had formed. H_2O (20 mL) was added, and the resultant suspension was stirred for 15 min. The suspension was filtered, then washed with H_2O (100 mL), followed by MeOH (100 mL) and finally Et_2O (100 mL). The solid was then dried in a vacuum oven at 40 °C for 12 h to give **14** as a white solid (323 mg, 70%). LCMS (formic method) retention time 0.51 min, $[M + H]^+ = 257$. 1H NMR (400 MHz, DMSO- d_6) δ ppm 3.79 (s, 2H), 7.25–7.31 (m, 1H), 7.36 (d, $J = 4.5$ Hz, 4H), 7.74 (d, $J = 5.1$ Hz, 1H), 8.41 (d, $J = 5.1$ Hz, 1H), 9.48 (s, 1H), 10.70 (br s, 1H).

3-Benzamidoisonicotinic Acid, 15. *Step 1.* Benzoyl chloride (91 μL , 0.78 mmol) was added to a stirred solution of ethyl 3-amino-4-pyridinecarboxylate (100 mg, 0.602 mmol) in DCM (3 mL) and sat. aq K_2CO_3 (3 mL) at rt. The resultant biphasic solution was stirred rapidly for 16 h, and then DCM (10 mL) and H_2O (20 mL) were added. The separated aqueous phase was extracted with DCM (2 \times 20 mL); the combined organic phases were passed through a hydrophobic frit and evaporated under reduced pressure to give a yellow oil. This oil was purified by MDAP (high pH method) to give a yellow solid (114 mg). The solid was further purified by MDAP (formic method) to give a pale yellow solid. The solid was dissolved in EtOH (10 mL) and loaded onto an amino propyl column (2 g) that had been prewashed with EtOH. The column was washed with EtOH, the fractions were combined and evaporated under reduced pressure to give ethyl 3-benzamidoisonicotinate as a pale yellow solid (72 mg, 44%). LCMS (formic method) retention time 1.01 min, $[M + H]^+ = 271$. 1H NMR (400 MHz, $CDCl_3$) δ ppm 1.50 (t, $J = 7.2$ Hz, 3H), 4.52 (q, $J = 7.0$ Hz, 2H), 7.53–7.67 (m, 3H), 7.90 (d, $J = 5.0$ Hz, 1H),

8.07–8.09 (m, 1H), 8.10 (s, 1H), 8.52 (d, $J = 5.0$ Hz, 1H), 10.29 (s, 1H), 11.71 (br s, 1H)

Step 2. Lithium hydroxide monohydrate (19 mg, 0.44 mmol) was added in a single portion to a stirred solution of ethyl 3-benzamidoisonicotinate (60 mg, 0.222 mmol) in THF (3 mL) and H₂O (1 mL) at rt. After stirring at rt for 2 h, 2 M HCl (aq) (2 mL) was added dropwise and the resultant suspension filtered. The filtered solid was washed with Et₂O (20 mL) and then dried under vacuum to give **15** as a white solid (31 mg, 58%). LCMS (formic method) retention time 0.51 min, $[M + H]^+ = 243$. ¹H NMR (400 MHz, DMSO-*d*₆) δ ppm 7.62 (t, $J = 7.8$ Hz, 2H), 7.68 (t, $J = 7.8$ Hz, 1H), 7.87 (d, $J = 5.0$ Hz, 1H), 7.99 (d, $J = 7.8$ Hz, 2H), 8.51 (d, $J = 5.0$ Hz, 1H), 9.69 (s, 1H), 11.66 (br s, 1H).

3-(3-Phenylpropanamido)isonicotinic Acid, 13. Compound **13** was prepared in a similar manner to compound **15**. LCMS (formic method) retention time 0.60 min, $[M + H]^+ = 271$. ¹H NMR (400 MHz, DMSO-*d*₆) δ ppm 2.73 (t, $J = 7.5$ Hz, 2H), 2.94 (t, $J = 7.5$ Hz, 2H), 7.16–7.22 (m, 1H), 7.24–7.32 (m, 4H), 7.75 (d, $J = 5.1$ Hz, 1H), 8.42 (d, $J = 5.1$ Hz, 1H), 9.38 (s, 1H), 10.61 (br s, 1H).

3-(Benzylamino)isonicotinic Acid, 17. **Step 1.** Sodium triacetox-yborohydride (383 mg, 1.805 mmol) was added portionwise over 0.5 min to a stirred suspension of ethyl 3-amino-4-pyridinecarboxylate (250 mg, 1.504 mmol), benzaldehyde (0.167 mL, 1.655 mmol), and trifluoroacetic acid (0.232 mL, 3.01 mmol) in isopropyl acetate (3 mL) at rt under N₂. After stirring at rt for 30 min, sat. NaHCO₃ (aq) (10 mL) was added slowly over 5 min. The biphasic solution was then diluted with sat. NaHCO₃ (aq) (20 mL) and EtOAc (20 mL). The separated aqueous phase was extracted with EtOAc (2 × 20 mL); the combined organics were passed through a hydrophobic frit and evaporated under reduced pressure to give an orange oil. This oil was purified by silica gel column chromatography using a gradient of 0–20% EtOAc/cyclohexane to give ethyl 3-(benzylamino)isonicotinate as a pale yellow oil (300 mg, 78%). LCMS (formic method) retention time 0.92 min, $[M + H]^+ = 257$. ¹H NMR (400 MHz, CDCl₃) δ ppm 1.42 (t, $J = 7.1$ Hz, 3H), 4.38 (q, $J = 7.3$ Hz, 2H), 4.54 (d, $J = 5.6$ Hz, 2H), 4.73 (d, $J = 5.8$ Hz, 1H), 7.29–7.35 (m, 1H), 7.36–7.42 (m, 4H), 7.68 (d, $J = 5.1$ Hz, 1H), 7.86 (br s, 1H), 7.94 (d, $J = 5.1$ Hz, 1H), 8.22 (s, 1H).

Step 2. Lithium hydroxide monohydrate (85 mg, 2.029 mmol) was added in a single portion to a stirred solution of ethyl 3-(benzylamino)isonicotinate (260 mg, 1.014 mmol) in THF (5 mL) and water (1.7 mL) at rt. The resultant suspension was stirred at rt for 16 h by which time a solution had formed. 2 M HCl (aq) (5 mL) was added, and the resultant suspension was stirred for 5 min. The suspension was filtered; the collected solid was washed with H₂O (50 mL) and Et₂O (50 mL) and dried under vacuum to give **17** as a pale yellow solid (44 mg, 19%). LCMS (formic method) retention time 0.51 min, $[M + H]^+ = 229$. ¹H NMR (400 MHz, DMSO-*d*₆) δ ppm 4.58 (s, 2H), 7.24–7.30 (m, 1H), 7.35–7.39 (m, 4H), 7.58 (d, $J = 5.1$ Hz, 1H), 7.83 (d, $J = 5.1$ Hz, 1H), 8.15 (s, 1H).

3-(Phenethylamino)isonicotinic Acid, 18. **Step 1.** Sodium triacetox-yborohydride (191 mg, 0.903 mmol) was added in a single portion to a stirred solution of ethyl 3-amino-4-pyridinecarboxylate (100 mg, 0.602 mmol) in trifluoroacetic acid (0.6 mL, 7.79 mmol) at rt. After stirring at rt for 10 min, a solution of phenylacetaldehyde (0.074 mL, 0.662 mmol) in DCM (1.2 mL) was added dropwise over 1 min. The resultant solution was stirred at rt for 30 min, and sodium triacetox-yborohydride (191 mg, 0.903 mmol) was added. The resultant solution was stirred at rt for 10 min, and then a solution of phenylacetaldehyde (0.074 mL, 0.662 mmol) in DCM (1.2 mL) was added dropwise over 1 min. The resultant solution was stirred at rt for 1 h. The solution was diluted with DCM and poured into sat. NaHCO₃ (aq) (50 mL). The separated aqueous phase was extracted with DCM; the combined organics were passed through a hydrophobic frit and evaporated under reduced pressure to give a yellow oil. The oil was purified by MDAP (formic method) to give a yellow oil. The oil was dissolved in EtOH (10 mL) and loaded onto an aminopropyl column (5 g) that had been prewashed with EtOH. The product was eluted with EtOH and the combined fractions were evaporated under reduced pressure to give ethyl 3-[(2-phenylethyl)-

amino]-4-pyridinecarboxylate as a colorless oil (95 mg, 58%). LCMS (formic method) retention time 0.94 min, $[M + H]^+ = 271$. ¹H NMR (400 MHz, CDCl₃) δ ppm 1.39 (t, $J = 7.2$ Hz, 3H), 3.02 (t, $J = 7.3$ Hz, 2H), 3.57 (td, $J = 7.2, 5.6$ Hz, 2H), 4.34 (q, $J = 7.2$ Hz, 2H), 7.25–7.31 (m, 3H), 7.35 (t, $J = 8.0$ Hz, 2H), 7.46 (m, 1H), 7.64 (d, $J = 5.1$ Hz, 1H), 7.92 (d, $J = 5.1$ Hz, 1H), 8.27 (s, 1H).

Step 2. Lithium hydroxide monohydrate (30 mg, 0.715 mmol) was added in a single portion to a stirred solution of ethyl 3-[(2-phenylethyl)amino]-4-pyridinecarboxylate (95 mg, 0.351 mmol) in THF (5 mL) and water (1.667 mL) at rt. The resultant suspension was stirred for 16 h. The reaction was then warmed to 50 °C for 30 min. Upon cooling, 2 M HCl (aq) (5 mL) was added and the solvent was evaporated under reduced pressure to give a yellow oil. The oil was suspended in MeOH (10 mL) and loaded onto an SCX column (5 g) that had been prewashed with MeOH. The column was washed with MeOH, then 2 M NH₃ in MeOH. The methanolic ammonia fractions were combined and evaporated under reduced pressure to give **18** as a yellow solid (74 mg, 87%). LCMS (formic method) retention time 0.56 min, $[M + H]^+ = 243$. ¹H NMR (400 MHz, DMSO-*d*₆) δ ppm 2.88 (t, $J = 7.3$ Hz, 2H), 3.39 (t, $J = 7.3$ Hz, 2H), 7.21 (td, $J = 5.8, 2.5$ Hz, 1H), 7.29–7.33 (m, 4H), 7.54 (d, $J = 4.8$ Hz, 1H), 7.70 (d, $J = 4.8$ Hz, 1H), 7.99 (s, 1H).

3-((3-Phenylpropyl)amino)isonicotinic Acid, 19. **Step 1.** Sodium triacetox-yborohydride (383 mg, 1.805 mmol) was added portionwise over 0.5 min to a stirred solution of ethyl 3-amino-4-pyridinecarboxylate (250 mg, 1.504 mmol), 3-phenylpropanal (0.218 mL, 1.655 mmol), and trifluoroacetic acid (0.695 mL, 9.03 mmol) in isopropyl acetate (3 mL) at rt under N₂. After stirring at rt for 30 min, sat. NaHCO₃ (aq) was added slowly over 5 min. The biphasic solution was then diluted with sat. NaHCO₃ (aq) and extracted with EtOAc. The organic phase was passed through a hydrophobic frit and evaporated to give an orange oil. This oil was purified using silica gel column chromatography eluting with a gradient of 0–20% EtOAc/cyclohexane to give ethyl 3-[(3-phenylpropyl)amino]-4-pyridinecarboxylate as a yellow oil (278 mg, 65%). LCMS (formic method) retention time 1.03 min, $[M + H]^+ = 285$.

Step 2. Lithium hydroxide monohydrate (74 mg, 1.764 mmol) was added in a single portion to a stirred solution of ethyl 3-[(3-phenylpropyl)amino]-4-pyridinecarboxylate (250 mg, 0.879 mmol) in THF (5 mL) and water (1.7 mL) at rt. The resultant suspension was stirred at rt for 16 h, and then 2 M HCl(aq) (5 mL) was added. The solvent was evaporated under reduced pressure to give a yellow solid. The solid was dissolved in MeOH (10 mL) and loaded onto an SCX column (5 g) that had been prewashed with MeOH. The column was then washed with MeOH, followed by 2 M NH₃ in MeOH. The methanolic ammonia fractions were combined and evaporated under reduced pressure to give **19** as a yellow solid (112 mg, 50%). LCMS (formic method) retention time 0.66 min, $[M + H]^+ = 257$. ¹H NMR (400 MHz, DMSO-*d*₆) δ ppm 1.88 (m, 2H), 2.70 (t, $J = 7.6$ Hz, 2H), 3.15 (t, $J = 7.0$ Hz, 2H), 7.18 (t, $J = 7.2$ Hz, 1H), 7.23 (d, $J = 7.2$ Hz, 2H), 7.29 (t, $J = 7.2$ Hz, 2H), 7.54 (d, $J = 4.8$ Hz, 1H), 7.69 (d, $J = 4.8$ Hz, 1H), 7.90 (s, 1H).

3-((4-Phenylbutyl)amino)isonicotinic Acid, 20. 4-Phenylbutan-1-amine (1.972 mL, 12.47 mmol) was added to a microwave vial containing 3-fluoroisonicotinic acid (800 mg, 5.67 mmol). The vial was sealed and then heated in a microwave at 150 °C for 2 h. The vial was allowed to stand at rt for 12 h. The viscous solution was dissolved in IPA (50 mL) and loaded onto an aminopropyl column (70 g) that had been prewashed with IPA. The column was washed with IPA and then 10% 2 M aq. HCl in IPA. The appropriate fractions were combined and evaporated under reduced pressure to give **20** as a yellow solid (1.23g, 70%). LCMS (formic method) retention time 0.72 min, $[M + H]^+ = 271$. ¹H NMR (400 MHz, DMSO-*d*₆) δ ppm 1.59–1.73 (m, 4H), 2.64 (t, $J = 7.2$ Hz, 2H), 3.37 (t, $J = 6.7$ Hz, 2H), 7.16 (d, $J = 7.2$ Hz, 1H), 7.21 (d, $J = 7.2$ Hz, 2H), 7.28 (t, $J = 7.4$ Hz, 2H), 7.96 (d, $J = 5.6$ Hz, 1H), 8.04 (d, $J = 5.8$ Hz, 1H), 8.39 (s, 1H).

3-(Propylamino)isonicotinic Acid, 21. 3-Fluoroisonicotinic acid (240 mg, 1.701 mmol) and propan-1-amine (0.156 mL, 1.871 mmol) were dissolved in NMP (1 mL) in a microwave vial. The mixture was then irradiated at 150 °C in a microwave for 4 h and then purified

using MDAP (formic method) to yield the **21** as a pale yellow powder (109 mg, 36%). LCMS (formic method) retention time 0.38 min, $[M + H]^+ = 181$. $^1\text{H NMR}$ (400 MHz, DMSO- d_6) δ ppm 0.96 (t, $J = 7.3$ Hz, 3H), 1.62 (m, 2H), 3.25 (t, $J = 7.0$ Hz, 2H), 7.55 (d, $J = 5.1$ Hz, 1H), 7.82 (d, $J = 5.1$ Hz, 1H), 8.24 (s, 1H).

3-(Butylamino)isonicotinic Acid, 22. To 3-fluoroisonicotinic acid (223 mg, 1.580 mmol) under nitrogen was added butan-1-amine (470 μL , 4.74 mmol), and the mixture was heated to 180 °C in a microwave for 4 h. The reaction mixture was diluted with DMSO and purified by MDAP (high pH method) to give **22** as a cream solid (10.4 mg, 3%). LCMS (formic method) retention time 0.47 min, $[M + H]^+ = 195$. $^1\text{H NMR}$ (400 MHz, DMSO- d_6) δ ppm 0.93 (t, $J = 7.3$ Hz, 3H), 1.40 (m, 2H), 1.60 (quin, $J = 7.2$ Hz, 2H), 3.25–3.28 (m, 2H), 7.54 (d, $J = 5.1$ Hz, 1H), 7.81 (d, $J = 5.1$ Hz, 1H), 8.22 (s, 1H).

3-(Isobutylamino)isonicotinic Acid, 23. *Step 1.* Sodium triacetoxyborohydride (478 mg, 2.257 mmol) was added portionwise over 0.5 min to a stirred solution of ethyl 3-amino-4-pyridinecarboxylate (250 mg, 1.504 mmol), 2-methylpropanal (0.151 mL, 1.655 mmol), and trifluoroacetic acid (1.500 mL, 19.47 mmol) in isopropyl acetate (3 mL) at rt under N_2 . After stirring at rt for 3 h, the reaction mixture was left to stand for 65 h. Saturated NaHCO_3 (aq) (10 mL) was added slowly over 5 min. The biphasic solution was then diluted with sat. NaHCO_3 (aq) (20 mL) and EtOAc (20 mL). The separated aqueous phase was extracted with EtOAc (2 \times 20 mL); the combined organic phases were passed through a hydrophobic frit and evaporated under reduced pressure to give a dark yellow oil. The oil was purified by silica gel column chromatography eluting with a gradient of 0–20% EtOAc/cyclohexane to give a yellow oil. The oil was further purified by MDAP (formic method) to give ethyl 3-[(2-methylpropyl)amino]-4-pyridinecarboxylate as a yellow oil (105 mg, 31%). LCMS (formic method) retention time 0.87 min, $[M + H]^+ = 223$. $^1\text{H NMR}$ (400 MHz, CDCl_3) δ ppm 1.05 (d, $J = 6.8$ Hz, 6H), 1.42 (t, $J = 7.1$ Hz, 3H), 2.00 (m, 1H), 3.12 (dd, $J = 6.6, 5.8$ Hz, 2H), 4.37 (q, $J = 7.2$ Hz, 2H), 7.50 (br s, 1H), 7.64 (d, $J = 5.3$ Hz, 1H), 7.90 (d, $J = 5.1$ Hz, 1H), 8.24 (s, 1H).

Step 2. Lithium hydroxide monohydrate (28 mg, 0.667 mmol) was added in a single portion to a stirred solution of ethyl 3-[(2-methylpropyl)amino]-4-pyridinecarboxylate (75 mg, 0.337 mmol) in THF (5 mL) and water (1.7 mL) at rt. The solution was stirred at rt for 21 h. 2 M HCl (aq) (5 mL) was added, and the resultant solution was stirred at rt for 10 min. The solvent was removed under reduced pressure to give a yellow oil. The sample was dissolved in MeOH and loaded onto a SCX-2 cartridge (5 g) that had been prewashed with methanol. The column was washed with MeOH and then eluted with 2 M NH_3 in MeOH. The appropriate fractions were combined and concentrated to give **23** as a yellow solid (53 mg, 81%). LCMS (formic method) retention time 0.50 min, $[M + H]^+ = 195$. $^1\text{H NMR}$ (400 MHz, MeOH- d_4) δ ppm 1.05 (d, $J = 6.8$ Hz, 6H), 1.97 (dt, $J = 13.3, 6.6$ Hz, 1H), 3.08 (d, $J = 6.8$ Hz, 2H), 7.77 (q, $J = 5.1$ Hz, 2H), 8.02 (s, 1H).

3-((2-Aminoethyl)amino)isonicotinic Acid, 24. 3-Fluoroisonicotinic acid (255 mg, 1.807 mmol) was suspended in ethylenediamine (1.5 mL, 22.44 mmol) and irradiated in a microwave at 150 °C for 2 h. The mixture was loaded on to a 5 g flash NH_2 column, then eluted with IPA (30 mL) and 2 M HCl (25 mL). The acidic fractions were evaporated to dryness, loaded on to a 10 g SCX cartridge, and eluted with water/MeOH (1:1) followed by 2 M NH_3 in MeOH. The basic fractions were evaporated to a white solid, and this was triturated with MeOH, filtered, and dried under reduced pressure to give **24** as a white solid (140 mg, 40%). LCMS (TFA method) retention time 0.18 min, $[M + H]^+ = 182$. $^1\text{H NMR}$ (400 MHz, D_2O) δ ppm 3.27 (t, $J = 5.9$ Hz, 2H), 3.62 (t, $J = 5.8$ Hz, 2H), 7.56 (d, $J = 5.1$ Hz, 1H), 7.90 (d, $J = 5.1$ Hz, 1H), 8.09 (s, 1H).

3-((3-Aminopropyl)amino)isonicotinic Acid, 25. *Step 1.* To a solution of 3-fluoroisonicotinic acid (400 mg, 2.83 mmol) in 1,4-dioxane (3 mL) was added *tert*-butyl (3-aminopropyl)carbamate (494 mg, 2.83 mmol), and the mixture was irradiated at 120 °C in a microwave for 36 h. The mixture was concentrated and the residue was purified by silica gel chromatography, eluting with a gradient of 0–10% MeOH in DCM to give 3-((3-((*tert*-butoxycarbonyl)amino)-

propyl)amino)isonicotinic acid (227 mg, 0.769 mmol, 27.1% yield) as a yellow oily solid. LCMS (TFA method) retention time 0.54 min, $[M + H]^+ = 296$. $^1\text{H NMR}$ (400 MHz, DMSO- d_6) δ ppm 1.37–1.40 (m, 9H), 1.69 (t, $J = 7.1$ Hz, 2H), 2.70 (s, 1H), 2.77 (m, 1H), 3.03 (q, $J = 6.7$ Hz, 2H), 7.54 (d, $J = 4.8$ Hz, 1H), 7.76 (d, $J = 5.1$ Hz, 1H), 8.10 (s, 1H).

Step 2. To a solution of 3-((3-((*tert*-butoxycarbonyl)amino)-propyl)amino)isonicotinic acid (45 mg, 0.152 mmol) in DCM (3 mL) was added trifluoroacetic acid (0.1 mL, 1.298 mmol), and the mixture was stirred at room temperature for 16 h. The solvent was removed under reduced pressure and the residue dissolved in MeOH. The solution was applied to a 5 g Isolute SCX cartridge, washing with MeOH (25 mL) and eluting with 2 M NH_3 in MeOH (25 mL). The solvent was removed under reduced pressure to give **25** (21 mg, 70.6% yield) as a pale yellow solid. LCMS (TFA method) retention time 0.21 min, $[M + H]^+ = 196$. $^1\text{H NMR}$ (400 MHz, D_2O) $\delta = 2.06$ –1.93 (m, 2H), 3.09 (t, $J = 7.6$ Hz, 2H), 3.39–3.30 (m, 2H), 7.54 (d, $J = 4.8$ Hz, 1H), 7.86 (d, $J = 4.8$ Hz, 1H), 8.07 (s, 1H).

3-((2,5-Dimethylbenzyl)amino)isonicotinic Acid Hydrochloride, 26. *Step 1.* To 3-fluoroisonicotinic acid (200 mg, 1.417 mmol) and *N*-ethyl-*N*-isopropylpropan-2-amine (619 μL , 3.54 mmol) was added (2,5-dimethylphenyl)methanamine (230 mg, 1.701 mmol) in a microwave vial. The reaction mixture was irradiated in a microwave for 4 h at 160 °C. The reaction mixture was diluted with 4 mL of DMSO and purified by MDAP (high pH method) to give 3-((2,5-dimethylbenzyl)amino)isonicotinic acid (178 mg, 49%) as a white solid. LCMS (high pH method) retention time 0.72 min, $[M + H]^+ = 257$. $^1\text{H NMR}$ (400 MHz, DMSO- d_6) $\delta = 2.23$ (s, 3H), 2.28 (s, 3H), 4.47 (s, 2H), 7.01 (d, $J = 7.6$ Hz, 1H), 7.10 (s, 1H), 7.10 (d, $J = 7.6$ Hz, 2H), 7.58 (d, $J = 5.1$ Hz, 1H), 7.85 (d, $J = 5.1$ Hz, 1H), 8.19 (s, 1H).

Step 2. To a solution of 3-((2,5-dimethylbenzyl)amino)isonicotinic acid (49.9 mg, 0.195 mmol) in 1,4-dioxane (4 mL) was added 2 M HCl in diethyl ether (0.097 mL, 0.195 mmol), and the solution was blown down to give **26** (56 mg, 49%). LCMS (high pH method) retention time 0.71 min, $[M + H]^+ = 257$. $^1\text{H NMR}$ (400 MHz, DMSO- d_6) δ ppm 2.23 (s, 3H), 2.29 (s, 3H), 7.03 (d, $J = 7.8$ Hz, 1H), 7.08 (s, 1H), 7.12 (d, $J = 7.6$ Hz, 1H), 7.97 (q, $J = 5.6$ Hz, 2H), 8.27 (s, 1H).

3-((2,3-Dimethylbenzyl)amino)isonicotinic Acid Hydrochloride, 27. *Step 1.* To 3-fluoroisonicotinic acid (200 mg, 1.417 mmol) and *N*-ethyl-*N*-isopropylpropan-2-amine (619 μL , 3.54 mmol) was added (2,3-dimethylphenyl)methanamine (230 mg, 1.701 mmol) in a microwave vial. The reaction was irradiated in a microwave for 4 h at 160 °C. The reaction was diluted with DMSO and purified by MDAP (high pH method) to give 3-((2,3-dimethylbenzyl)amino)isonicotinic acid (139.2 mg, 38%) as a white solid. LCMS (high pH method) retention time 0.71 min, $[M + H]^+ = 257$. $^1\text{H NMR}$ (400 MHz, DMSO- d_6) δ ppm 2.22 (s, 3 H), 2.28 (s, 3 H), 4.52 (s, 2 H), 7.02–7.14 (m, 3 H), 7.58 (d, $J = 5.1$ Hz, 1 H), 7.84 (d, $J = 5.1$ Hz, 1H), 8.19 (s, 1 H).

Step 2. To a solution of 3-((2,3-dimethylbenzyl)amino)isonicotinic acid (51.1 mg, 0.199 mmol) in 1,4-dioxane (4 mL) was added 2 M HCl in 1,4-dioxane (0.100 mL, 0.199 mmol). The solution was blown down and dried under vacuum to give **27** (55.2 mg, 95%) as a light yellow solid. LCMS (high pH method) retention time 0.71 min, $[M + H]^+ = 257$. $^1\text{H NMR}$ (400 MHz, DMSO- d_6) δ ppm 2.22 (s, 3H), 2.28 (s, 3H), 4.56 (s, 2H), 7.06 (t, $J = 7.5$ Hz, 1H), 7.10–7.14 (m, 2H), 7.88 (d, $J = 5.6$ Hz, 1H), 7.95 (d, $J = 5.6$ Hz, 1H), 8.27 (s, 1H).

3-((1,1'-Biphenyl)-3-ylmethyl)amino)isonicotinic Acid, 28. In a 10 mL vial, 3-fluoro-4-pyridinecarboxylic acid (100 mg, 0.70 mmol) and 3-phenylbenzylamine (129 mg, 0.070 mmol) were taken up in THF (0.5 mL) and stirred at –78 °C under N_2 . LiHMDS (1 M in THF) (3.9 mL, 3.90 mmol) was added, and the reaction was stirred at –78 °C for 15 min and then at rt for 16 h. The reaction was treated with 2 M NaOH (2 mL) and stirred at rt for 24 h. The reaction was concentrated and triturated with ether, and the resulting solid was purified by HPLC to yield **28** (14 mg, 6%). LCMS (formic method) retention time 0.78 min, $[M + H]^+ = 305$. $^1\text{H NMR}$ (400 MHz, DMSO- d_6) δ 4.60 (s, 2H), 7.35 (t, $J = 4$ Hz, 2H), 7.40 (q, $J = 8$ Hz,

2H), 7.55 (t, $J = 4$ Hz, 2H), 7.60 (d, $J = 12.0$ Hz, 2H), 7.68 (s, 2H), 7.8 (d, $J = 8.0$ Hz, 1H), 8.18 (s, 1H).

3-((Cyclohexylmethyl)amino)isonicotinic Acid, 29. A microwave vial was charged with 3-fluoroisonicotinic acid (200 mg, 1.417 mmol), cyclohexylmethanamine (0.276 mL, 2.126 mmol), and *N*-ethyl-*N*-isopropylpropan-2-amine (0.370 mL, 2.126 mmol) in IPA (4 mL). The reaction was irradiated in a microwave at 150 °C for 5 h. After cooling, the solvent was evaporated affording an orange oil. The sample was purified using silica gel column chromatography, eluting with a gradient of 0–50% EtOAc/cyclohexane followed by 0–20% MeOH/DCM to give crude title compound as an orange solid. This was taken up in MeOH and a precipitate formed which was removed by filtration and dried to give an orange solid. The crude orange solid was further purified by MDAP (formic method) to give **29** (7 mg, 2%) as a yellow solid. LCMS (formic method) retention time 0.66 min, $[M + H]^+ = 235$. ^1H NMR (400 MHz, DMSO- d_6) δ ppm 1.00 (m, 2H), 1.11–1.29 (m, 3H), 1.52–1.61 (m, 1H), 1.64 (d, $J = 10.5$ Hz, 1H), 1.67–1.73 (m, 2H), 1.78 (d, $J = 13.2$ Hz, 2H), 3.10 (d, $J = 6.6$ Hz, 2H), 7.54 (d, $J = 4.9$ Hz, 1H), 7.76 (d, $J = 4.9$ Hz, 1H), 8.14 (s, 1H).

3-((Cyclopentylmethyl)amino)isonicotinic Acid, 30. To 3-fluoroisonicotinic acid (200 mg, 1.417 mmol) under nitrogen were added *N*-ethyl-*N*-isopropylpropan-2-amine (619 μL , 3.54 mmol, IPA (619 μL), and cyclopentylmethanamine hydrochloride (231 mg, 1.701 mmol), and the mixture was irradiated in a microwave at 180 °C for 4 h. The reaction mixture was diluted with DMSO and purified by MDAP (high pH method) to give **30** (32 mg, 9%) as a yellow solid. LCMS (high pH method) retention time 0.58 min, $[M + H]^+ = 221$. ^1H NMR (400 MHz, DMSO- d_6) δ ppm 1.22–1.32 (m, 2H), 1.51–1.59 (m, 2H), 1.62 (d, $J = 6.6$ Hz, 2H), 1.73–1.82 (m, 2H), 2.18 (m, 1H), 3.19 (d, $J = 7.1$ Hz, 2H), 7.54 (d, $J = 5.1$ Hz, 1H), 7.80 (d, $J = 5.1$ Hz, 1H), 8.21 (s, 1H).

3-((Cyclopropylmethyl)amino)isonicotinic Acid, 31. To 3-fluoroisonicotinic acid (199 mg, 1.410 mmol) were added cyclopropylmethanamine (147 μL , 1.692 mmol) and *N*-ethyl-*N*-isopropylpropan-2-amine (614 μL , 3.53 mmol). The mixture was irradiated at 180 °C in the microwave for 4 h. The reaction was diluted with MeOH and purified by MDAP (formic method) to give **31** (67 mg, 95%) as a pale yellow solid. LCMS (formic method) retention time 0.40 min, $[M + H]^+ = 193$. ^1H NMR (400 MHz, DMSO- d_6) δ ppm 0.25–0.30 (m, 2H), 0.50–0.55 (m, 2H), 2.33 (s, 1H), 3.16 (d, $J = 6.8$ Hz, 2H), 7.55 (d, $J = 5.0$ Hz, 1H), 7.82 (d, $J = 5.0$ Hz, 1H), 8.23 (s, 1H).

3-((Thiophen-2-ylmethyl)amino)isonicotinic Acid, 32. In a microwave vial, to 3-fluoroisonicotinic acid (200 mg, 1.417 mmol) and *N*-ethyl-*N*-isopropylpropan-2-amine (619 μL , 3.54 mmol) was added thiophen-2-ylmethanamine (194 μL , 1.701 mmol). The reaction was irradiated in a microwave for 4 h at 160 °C. The reaction mixture was diluted with DMSO and purified by MDAP (high pH method) to give **32** as a light yellow solid (146 mg, 42%). LCMS (high pH method) retention time 0.53 min, $[M + H]^+ = 235$. ^1H NMR (400 MHz, DMSO- d_6) δ ppm 4.76 (s, 2H), 7.00 (m, 1H), 7.10 (d, $J = 2.5$ Hz, 1H), 7.41 (d, $J = 5.1$ Hz, 1H), 7.57 (d, $J = 5.1$ Hz, 1H), 7.85 (d, $J = 5.1$ Hz, 1H), 8.27 (s, 1H).

3-((Thiophen-3-ylmethyl)amino)isonicotinic Acid Hydrochloride, 33. In a microwave vial, to 3-fluoroisonicotinic acid (200 mg, 1.417 mmol) and *N*-ethyl-*N*-isopropylpropan-2-amine (619 μL , 3.54 mmol) was added thiophen-3-ylmethanamine (198 mg, 1.701 mmol). The reaction was irradiated in a microwave for 4 h at 160 °C. The reaction mixture was diluted with DMSO and purified by MDAP (high pH method) to give a white solid (83 mg). This solid was dissolved in 1,4-dioxane (3 mL), and 2 M HCl in ether (178 μL , 0.356 mmol) was added; the solution was evaporated and the resultant solid was dried under high vacuum to give **33** as a yellow solid (92.3 mg, 24%). LCMS (high pH method) retention time 0.55 min, $[M + H]^+ = 235$. ^1H NMR (400 MHz, DMSO- d_6) δ ppm 4.62 (s, 2H), 7.13 (dd, $J = 4.8, 1.0$ Hz, 1H), 7.45 (d, $J = 2.0$ Hz, 1H), 7.55 (dd, $J = 4.9, 2.9$ Hz, 1H), 7.99 (q, $J = 5.6$ Hz, 2H), 8.33 (s, 1H).

3-((Furan-2-ylmethyl)amino)isonicotinic Acid Hydrochloride, 34. To 3-fluoroisonicotinic acid (200 mg, 1.417 mmol) and *N*-ethyl-*N*-isopropylpropan-2-amine (619 μL , 3.54 mmol) was added

furan-2-ylmethanamine (157 μL , 1.701 mmol) in a microwave vial. The reaction mixture was irradiated in a microwave for 4 h at 160 °C. The reaction mixture was diluted with DMSO and purified by MDAP (high pH method) to give a white solid (31.1 mg). This solid was dissolved in 1,4-dioxane (2 mL), and 2 M HCl in Et₂O (71.3 μL , 0.142 mmol) was added to the solution. The solution was concentrated and dried to give **34** as a yellow solid (36.7 mg, 10%). LCMS (high pH method) retention time 0.49 min, $[M + H]^+ = 219$. HRMS: C₁₁H₁₁N₂O₃ requires $(M + H)^+ 219.0764$, found 219.0758 (error -2.7 ppm). ^1H NMR (400 MHz, DMSO- d_6) δ ppm 4.64 (br s, 2H), 6.41 (d, $J = 5.1$ Hz, 2H), 7.62 (br s, 1H), 7.91 (br. d, $J = 4.8$ Hz, 1H), 7.99 (m, 1H), 8.45 (br s, 1H). ^{13}C NMR (126 MHz, DMSO- d_6) δ ppm 169.3, 152.5, 144.6, 143.0, 136.4, 136.4, 123.7, 116.4, 110.9, 107.9, 39.4. Mp 242–245 °C.

3-((Thiazol-4-ylmethyl)amino)isonicotinic Acid, 35. 3-Aminoisonicotinic acid (30 mg, 0.217 mmol) was dissolved in MeOH (1.5 mL). To this was added thiazole-4-carbaldehyde (49 mg, 0.434 mmol), and the reaction mixture was stirred at rt for 10 min. NaCNBH₃ (27 mg, 0.434 mmol) was then added, and the reaction mixture was stirred for a further 18 h. The solvent was then evaporated and the residue was purified by reverse phase column chromatography, eluting with a gradient of acetonitrile in water (0–100%) to give **35** (10 mg, 20%) as a white solid. LCMS (high pH method) retention time 0.31 min, $[M + H]^+ = 236$. ^1H NMR (400 MHz, DMSO- d_6) δ ppm 4.67 (s, 2H), 7.59–7.51 (m, 2H), 7.83 (d, $J = 5.0$ Hz, 1H), 8.28 (s, 1H), 9.09 (d, $J = 2.0$ Hz, 1H), 13.39 (b. s, 1H).

3-(((1*H*-Pyrazol-5-yl)methyl)amino)isonicotinic acid, 36. In a microwave vial, to 3-fluoroisonicotinic acid (200 mg, 1.417 mmol) and (1*H*-pyrazol-5-yl)methanamine dihydrochloride (289 mg, 1.701 mmol) was added *N*-ethyl-*N*-isopropylpropan-2-amine (617 μL , 3.54 mmol). The reaction was irradiated in a microwave for 4 h at 160 °C. The reaction mixture was diluted with DMSO and purified by MDAP (high pH method) to give **36** as a yellow solid (28 mg, 9%). LCMS (high pH method) retention time 0.35 min, purity 86%, $[M + H]^+ = 219$. ^1H NMR (400 MHz, DMSO- d_6) δ ppm 4.47 (s, 2H), 6.20 (d, $J = 2.0$ Hz, 1H), 7.55 (d, $J = 4.9$ Hz, 1H), 7.61 (br s, 1H), 7.81 (d, $J = 4.9$ Hz, 1H), 8.24 (s, 1H).

3-(((5-Methylthiophen-2-yl)methyl)amino)isonicotinic Acid Hydrochloride, 37. To 3-fluoroisonicotinic acid (200 mg, 1.417 mmol) and *N*-ethyl-*N*-isopropylpropan-2-amine (0.619 mL, 3.54 mmol) was added (5-methylthiophen-2-yl)methanamine (0.219 mL, 1.701 mmol) in a microwave vial. The reaction mixture was irradiated in a microwave for 4 h at 160 °C. The reaction mixture was diluted with DMSO and purified by MDAP (high pH method) to give a white solid (74.2 mg). This solid was dissolved in 1,4-dioxane (3 mL), and 2 M HCl in Et₂O (0.149 mL, 0.298 mmol) was added. The mixture was blown down and dried under reduced pressure to give **37** as a yellow solid (82.4 mg, 20%). LCMS (high pH method) retention time 0.62 min, $[M + H]^+ = 249$. ^1H NMR (400 MHz, DMSO- d_6) δ ppm 2.39 (s, 3H), 4.74 (s, 2H), 6.67 (d, $J = 2.3$ Hz, 1H), 6.92 (d, $J = 3.3$ Hz, 1H), 8.00 (s, 2H), 8.39 (s, 1H).

3-(((4-Methylthiophen-2-yl)methyl)amino)isonicotinic Acid, 38. In a microwave vial, to 3-fluoroisonicotinic acid (200 mg, 1.417 mmol) and (4-methylthiophen-2-yl)methanamine (216 mg, 1.701 mmol) was added *N*-ethyl-*N*-isopropylpropan-2-amine (617 μL , 3.54 mmol). The reaction was irradiated in a microwave for 4 h at 160 °C. The reaction mixture was diluted with DMSO and purified by MDAP (high pH method) to give the **38** as a light yellow solid (69.8 mg, 20%). LCMS (high pH method) retention time 0.61 min, $[M + H]^+ = 249$. ^1H NMR (400 MHz, DMSO- d_6) δ ppm 2.16 (s, 3H), 4.68 (s, 2H), 6.91 (s, 1H), 6.97 (s, 1H), 7.57 (d, $J = 4.9$ Hz, 1H), 7.84 (d, $J = 5.1$ Hz, 1H), 8.24 (s, 1H).

3-(((3-Methylthiophen-2-yl)methyl)amino)isonicotinic Acid, 39. To 3-fluoroisonicotinic acid (200 mg, 1.417 mmol) and *N*-ethyl-*N*-isopropylpropan-2-amine (0.619 mL, 3.54 mmol) was added (3-methylthiophen-2-yl)methanamine (216 mg, 1.701 mmol) in a microwave vial. The reaction mixture was heated for 4 h at 160 °C in a microwave. The reaction mixture was diluted with DMSO (2 mL) and purified by MDAP (high pH method) to give **39** as a light yellow solid (40 mg, 11%). LCMS (formic method) retention time 0.54 min,

$[M + H]^+ = 249$. HRMS: $C_{12}H_{12}N_2O_2S$ requires $[M + H]^+ 249.0692$, found 249.0692 (error 0.1 ppm). 1H NMR (400 MHz, DMSO- d_6) δ ppm 2.24 (s, 3H), 4.69 (s, 2H), 6.89 (d, $J = 4.9$ Hz, 1H), 7.33 (d, $J = 5.1$ Hz, 1H), 7.83 (d, $J = 5.1$ Hz, 1H), 7.96 (d, $J = 5.1$ Hz, 1H), 8.31 (s, 1H). ^{13}C NMR (126 MHz, DMSO- d_6) δ ppm 169.9, 164.0, 144.7, 136.5, 136.2, 135.2, 134.0, 130.7, 124.3, 123.5, 121.8, 13.8. Mp 238–241 °C.

3-((Benzo[*b*]thiophen-2-ylmethyl)amino)isonicotinic Acid, 40. 3-Aminoisonicotinic acid (20 mg, 0.153 mmol) was dissolved in MeOH (1 mL). To this was added benzo(*b*)thiophene 7-carbaldehyde (49 mg, 0.305 mmol) and NaCNBH₃ (20 mg, 0.305 mmol), and the reaction mixture was stirred for 18 h at rt. The solvent was evaporated and the residue was purified by reverse phase column chromatography, eluting with a gradient of acetonitrile in water (0–100%) to give **40** (14 mg, 32%) as a white solid. 1H NMR (400 MHz, DMSO- d_6) δ 4.69 (s, 2H), 7.32–7.22 (m, 2H), 7.33 (s, 1H), 7.52 (dd, $J = 4.7, 1.1$ Hz, 1H), 7.68 (dd, $J = 4.7, 1.2$ Hz, 1H), 7–7.5 (d, $J = 7.9$ Hz, 1H), 7.86 (d, $J = 7.9$ Hz, 1H), 7.94 (s, 1H), 9.68 (br s, 1H).

3-((1-Phenylethyl)amino)isonicotinic Acid, 41. To 3-fluoroisonicotinic acid (200 mg, 1.417 mmol) under nitrogen was added 1-phenylethylamine (548 μ L, 4.25 mmol), and the mixture was irradiated at 180 °C in a microwave for 4 h. The reaction mixture was diluted with DMSO and purified by MDAP (high pH method) to give **41** as a cream solid (204 mg, 54%). LCMS (formic method) retention time 0.56 min, $[M + H]^+ = 243$. 1H NMR (400 MHz, DMSO- d_6) δ ppm 1.47 (d, $J = 6.6$ Hz, 3H), 4.73 (q, $J = 6.6$ Hz, 1H), 7.21 (t, $J = 7.5$ Hz, 1H), 7.32 (t, $J = 7.5$ Hz, 2H), 7.37 (d, $J = 8.0$ Hz, 2H), 7.55 (d, $J = 4.8$ Hz, 1H), 7.69 (d, $J = 4.8$ Hz, 1H), 7.79 (s, 1H).

3-((2-Phenylpropan-2-yl)amino)isonicotinic Acid, 42. To a solution of 3-fluoroisonicotinic acid (100 mg, 0.709 mmol) in NMP (0.25 mL) under nitrogen was added 2-phenylpropan-2-amine (105 mg, 0.780 mmol) and *N*-ethyl-*N*-isopropylpropan-2-amine (0.149 mL, 0.850 mmol). The mixture was irradiated at 180 °C in the microwave for 12 h. The reaction mixture was diluted with MeOH and purified by MDAP (high pH method) to give **42** (9 mg, 4%) as a cream powder. LCMS (formic method) retention time 0.59 min, $[M + H]^+ = 257$. 1H NMR (400 MHz, DMSO- d_6) δ ppm 1.65 (s, 6H), 7.24 (t, $J = 7.5$ Hz, 1H), 7.35 (t, $J = 7.6$ Hz, 3H), 7.45 (d, $J = 7.6$ Hz, 2H), 7.57 (d, $J = 4.6$ Hz, 1H), 7.64 (d, $J = 4.6$ Hz, 1H), 8.19 (s, 1H).

3-(Benzhydrylamino)isonicotinic Acid, 43. 1,1-Diphenylmethanamine (1.526 mL, 8.86 mmol) was added in a single portion to a stirred suspension of 3-fluoro-4-pyridinecarboxylic acid (250 mg, 1.772 mmol) and *N*-ethyl-*N*-isopropylpropan-2-amine (0.619 mL, 3.54 mmol) at rt. The reaction was irradiated in a microwave at 150 °C for 4 h. The crude reaction was diluted in DMSO and purified by MDAP (high pH method) to give **43** as a white solid (9 mg, 2%). LCMS (formic method) retention time 0.76 min, $[M + H]^+ = 305$. 1H NMR (400 MHz, DMSO- d_6) δ ppm 6.04 (d, $J = 4.0$ Hz, 1H), 7.27 (t, $J = 7.3$ Hz, 2H), 7.37 (t, $J = 7.3$ Hz, 4 H), 7.42 (d, $J = 7.3$ Hz, 4 H), 7.61 (d, $J = 5.1$ Hz, 1H), 7.85 (d, $J = 5.1$ Hz, 1H), 8.07 (s, 1H), 8.31 (br s, 1H).

2-((Furan-2-ylmethyl)amino)nicotinic Acid, 44. *Step 1.* Methyl 2-bromonicotinate (300 mg, 1.38 mmol) was dissolved in 1,4-dioxane (5 mL) under nitrogen. To this was added furan-2-ylmethanamine (161 mg, 1.66 mmol), Xantphos (160 mg, 0.28 mmol), Pd₂(dba)₃ (127 mg, 0.14 mmol), and Cs₂CO₃ (1.13 g, 3.47 mmol). The reaction mixture was then heated to 90 °C for 3 h. The reaction was diluted with EtOAc and washed with water. The combined organics were then dried over Na₂SO₄, filtered, and evaporated. The residue was then purified by column chromatography, eluting with 0–100% EtOAc/cyclohexane to give methyl 2-((furan-2-ylmethyl)amino)nicotinate (233 mg, 73%).

Step 2. Methyl 2-((furan-2-ylmethyl)amino)nicotinate (233 mg, 1.00 mmol) was dissolved in THF (2 mL), and to this was added a solution of NaOH (60 mg, 1.50 mmol) in water (2 mL). The reaction mixture was stirred at room temperature for 18 h and then acidified with 5% NaHSO₄ (aq). This was then extracted with EtOAc, and the combined organic phases were dried over Na₂SO₄, filtered and evaporated. The residue was then purified by reverse phase column chromatography, eluting with a gradient of 0–100% acetonitrile with 0.2% NH₃ in water to give **44** (56 mg, 26% yield) as a beige solid.

LCMS (formic method) retention time 0.48 min, $[M + H]^+ = 219$. HRMS: $C_{11}H_{11}N_2O_3$ requires $[M + H]^+ 219.0764$, found 219.0764 (error 0.0 ppm). 1H NMR (400 MHz, DMSO- d_6) δ ppm 4.66 (s, 2H), 6.25 (d, $J = 3.2$ Hz, 1H), 6.37 (m, 1H), 6.68–6.56 (m, 1H), 7.57 (d, $J = 1.7$ Hz, 1H), 8.07 (d, $J = 7.8$ Hz, 1H), 8.26 (d, $J = 4.7$ Hz, 1H), 8.35 (s, 1H), 13.14 (s, 1H). ^{13}C NMR (126 MHz, DMSO- d_6) δ ppm 169.3, 158.3, 153.6, 153.3, 142.6, 140.6, 112.1, 110.9, 107.1, 107.0, 37.6. Mp 197–202 °C.

2-(((3-Methylthiophen-2-yl)methyl)amino)nicotinic Acid, 45. *Step 1.* Methyl 2-bromonicotinate (0.3 g, 1.38 mmol, 1.0 equiv) was dissolved in 1,4-dioxane (5 mL) under nitrogen. To this was added (3-methylthiophen-2-yl)methanamine (0.212 g, 1.66 mmol), Xantphos (0.161 g, 0.28 mmol), Pd₂(dba)₃ (0.127 g, 0.14 mmol), and Cs₂CO₃ (1.13 g, 3.47 mmol). The reaction mixture was then heated to 90 °C for 3 h. The reaction was diluted with EtOAc and washed with water. The organic phase was dried over Na₂SO₄, filtered, and evaporated. The residue was purified by column chromatography, eluting with 0–100% EtOAc/cyclohexane to give methyl 2-(((methylthiophen-2-yl)methyl)amino)nicotinate (282 mg, 78%).

Step 2. Methyl 2-(((methylthiophen-2-yl)methyl)amino)nicotinate (282 mg, 1.08 mmol) was dissolved in THF (2 mL), and to this was added a solution of NaOH (64 mg, 1.61 mmol) in water (2 mL). The reaction mixture was stirred at room temperature for 18 h and then acidified with 5% NaHSO₄ (aq). The precipitate was collected by filtration, washed with water and EtOAc, then dried to give **45** (101 mg, 38%) as a cream solid. LCMS (formic method) retention time 0.69 min, $[M + H]^+ = 249$. HRMS: $C_{12}H_{12}N_2O_2S$ requires $[M + H]^+ 249.0692$, found 249.0692 (error 0.1 ppm). 1H NMR (400 MHz, DMSO- d_6) δ ppm 2.21 (s, 3H), 4.73 (s, 2H), 6.63 (m, 1H), 6.82 (d, $J = 5.0$ Hz, 1H), 7.24 (d, $J = 5.0$ Hz, 1H), 8.07 (d, $J = 7.6$ Hz, 1H), 8.27 (d, $J = 4.7$ Hz, 1H), 8.38 (s, 1H), 12.96 (s, 1H). ^{13}C NMR (126 MHz, DMSO- d_6) δ ppm 169.3, 158.1, 153.6, 140.6, 136.3, 134.0, 130.4, 123.4, 112.1, 106.8, 37.5, 13.8. Mp 223–226 °C.

■ ASSOCIATED CONTENT

● Supporting Information

The Supporting Information is available free of charge on the ACS Publications website at DOI: 10.1021/acs.jmedchem.5b01537.

Figure of putative prodrug **20E**; comparison of differential activity between KDM4C RFMS biochemical and cell imaging assays (ΔpIC_{50}) with compound lipophilicity; LCMS spectra and selectivity profiling data for **34** and **39**; methods for the KDM5C RFMS, EGLN3 HTRF, KDM4C cellular imaging and KDM5C cellular imaging assays; X-ray crystallography methods and data for **12** bound to KDM6B and KDM4D constructs and for **17** and **38** bound to KDM4D (PDF)
Molecular formula strings (CSV)

Accession Codes

X-ray crystal structures have been deposited in the Protein Data Bank as follows: compound **12** bound to KDM6B, PDB code SFP3; compound **12** bound to KDM4D, PDB code SFP4; compound **17** bound to KDM4D, PDB code SFP7; compound **38** bound to KDM4D, PDB code SFP8.

■ AUTHOR INFORMATION

Corresponding Authors

*S.M.W.: e-mail, sue.m.westaway@gsk.com; telephone, +44 (0) 1438763469.

*A.G.S.P.: e-mail, alex.gs.preston@gsk.com; telephone +44 (0) 1438790152.

Present Addresses

^{||}R.J.S. and D.M.W.: Oncology Innovative Medicines and Early Development, AstraZeneca, Cambridge Science Park, Milton Road, Cambridge CB4 0WG, U.K.

[⊥]K.L.: Bicycle Therapeutics Limited, Meditrina Building, Babraham Research Campus, Cambridge CB22 3AT, U.K.

[#]L.K.: Takeda Pharmaceuticals, 10275 Science Center Drive, San Diego, CA 92121, U.S.

Notes

The authors declare the following competing financial interest(s): All authors were GlaxoSmithKline and Cellzome full-time employees at the time this work was carried out.

ACKNOWLEDGMENTS

The authors thank Aymeric Bencib and Pradip Songara for synthetic chemistry contributions; Michael Woodrow and Neil Garton for medicinal chemistry logistical assistance; Shenaz Bunally for ChromLogD determination; Bill Leavens for HRMS analysis; Argyrides Argyrou, Anshu Bhardwaja, Angela Bridges, Matthew Burns, Rachel Grimley, Michelle Heathcote, Thau Ho, Jon Hutchinson, Sue Hutchinson, Emma Jones, John Martin, Lisa Miller, Linda Myers, Kelvin Nurse, Steve Ratcliffe, Mike Rees, Anthony Shillings, Kate Simpson, Penny Smee, Rob Tanner, Laura Williams, and Huizhen Zhao for assay reagent production, development, management, and data generation.

ABBREVIATIONS USED

KDM, lysine demethylase; JMJD, Jumonji C domain-containing protein; RFMS, RapidFire mass spectrometry; HTRF, homogeneous time-resolved fluorescence; JARID, Jumonji AT-rich interactive domain; 2-OG, 2-oxoglutarate; EGLN, egg-laying deficiency protein ninelike protein; PHD, prolyl hydroxylase domain protein; SCX, strong cation exchange; IPA, isopropyl alcohol

REFERENCES

- (1) Arrowsmith, C. H.; Bountra, C.; Fish, P. V.; Lee, K.; Schapira, M. Epigenetic protein families: a new frontier for drug discovery. *Nat. Rev. Drug Discovery* **2012**, *11*, 384–400.
- (2) Prinjha, R.; Tarakhovskiy, A. Chromatin targeting drugs in cancer and immunity. *Genes Dev.* **2013**, *27*, 1731–1738.
- (3) Lora, J. M.; Wilson, D. M.; Lee, K.; Larminie, C. G. C. Epigenetic control of the immune system: histone demethylation as a target for drug discovery. *Drug Discovery Today: Technol.* **2010**, *7*, e67–e75.
- (4) Black, J. C.; Van Rechem, C.; Whetstone, J. R. Histone lysine methylation dynamics: Establishment, regulation, and biological impact. *Mol. Cell* **2012**, *48*, 491–507.
- (5) Copeland, R. A.; Solomon, M. E.; Richon, V. M. Protein methyltransferases as a target class for drug discovery. *Nat. Rev. Drug Discovery* **2009**, *8*, 724–732.
- (6) Lohse, B.; Kristensen, J. L.; Kristensen, L. H.; Agger, K.; Helin, K.; Gajhede, M.; Clausen, R. P. Inhibitors of histone demethylases. *Bioorg. Med. Chem.* **2011**, *19*, 3625–3636.
- (7) Cloos, P. A.; Christensen, J.; Agger, K.; Maiolica, A.; Rappsilber, J.; Antal, T.; Hansen, K. H.; Helin, K. The putative oncogene GASC1 demethylates tri- and dimethylated lysine 9 on histone H3. *Nature* **2006**, *442*, 307–311.
- (8) Hamada, S.; Kim, T. D.; Suzuki, T.; Itoh, Y.; Tsumoto, H.; Nakagawa, H.; Janknecht, R.; Miyata, N. Synthesis and activity of N-oxalylglycine and its derivatives as Jumonji C-domain containing histone lysine demethylase inhibitors. *Bioorg. Med. Chem. Lett.* **2009**, *19*, 2852–2855.
- (9) Rose, N. R.; Woon, E. C.; Kingham, G. L.; King, O. N.; Mecnović, J.; Clifton, I. J.; Ng, S. S.; Talib-Hardy, J.; Oppermann, U.; McDonough, M. A.; Schofield, C. J. Selective inhibitors of the JMJD2

histone demethylases: combined nondenaturing mass spectrometric screening and crystallographic approaches. *J. Med. Chem.* **2010**, *53*, 1810–1818.

(10) Rose, N. R.; Ng, S. S.; Mecnović, J.; Liénard, B. M. R.; Bello, S. H.; Sun, Z.; McDonough, M. A.; Oppermann, U.; Schofield, C. J. Inhibitor scaffolds for 2-oxoglutarate-dependent histone lysine demethylases. *J. Med. Chem.* **2008**, *51*, 7053–7056.

(11) Chang, K. H.; King, O. N.; Tumber, A.; Woon, E. C.; Heightman, T. D.; McDonough, M. A.; Schofield, C. J.; Rose, N. R. Inhibition of histone demethylases by 4-carboxy-2,2'-bipyridyl compounds. *ChemMedChem* **2011**, *6* (5), 759–764.

(12) Thalhammer, A.; Mecnović, J.; Loenarz, C.; Tumber, A.; Rose, N. R.; Heightman, T. D.; Schofield, C. J. Inhibition of the histone demethylase JMJD2E by 3-substituted pyridine 2,4-dicarboxylates. *Org. Biomol. Chem.* **2011**, *9*, 127–135.

(13) Hopkinson, R. J.; Tumber, A.; Yapp, C.; Chowdhury, R.; Aik, W.; Che, K. H.; Li, X. S.; Kristensen, J. B. L.; King, O. N. F.; Chan, M. C.; Yeoh, K. K.; Choi, H.; Walport, L. J.; Thinnis, C. C.; Bush, J. T.; Lejeune, C.; Rydzik, A. M.; Rose, N. R.; Bagg, E. A.; McDonough, M. A.; Krojer, T. J.; Yue, W. W.; Ng, S. S.; Olsen, L.; Brennan, P. E.; Oppermann, U.; Müller, S.; Klose, R. J.; Ratcliffe, P. J.; Schofield, C. J.; Kawamura, A. 5-Carboxy-8-hydroxyquinoline is a broad spectrum 2-oxoglutarate oxygenase inhibitor which causes iron translocation. *Chem. Sci.* **2013**, *4*, 3110–3117.

(14) Rose, N. R.; Woon, E. C.; Tumber, A.; Walport, L. J.; Chowdhury, R.; Li, X. S.; King, O. N.; Lejeune, C.; Ng, S. S.; Krojer, T.; Chan, M. C.; Rydzik, A. M.; Hopkinson, R. J.; Che, K. H.; Daniel, M.; Strain-Damerell, C.; Gileadi, C.; Kochan, G.; Leung, I. K.; Dunford, J.; Yeoh, K. K.; Ratcliffe, P. J.; Burgess-Brown, N.; von Delft, F.; Müller, S.; Marsden, B.; Brennan, P. E.; McDonough, M. A.; Oppermann, U.; Klose, R. J.; Schofield, C. J.; Kawamura, A. Plant growth regulator daminozide is a selective inhibitor of human KDM2/7 histone demethylases. *J. Med. Chem.* **2012**, *55*, 6639–6643.

(15) Luo, X.; Liu, Y.; Kubicek, S.; Myllyharju, J.; Tumber, A.; Ng, S.; Che, K. H.; Podoll, J.; Heightman, T. D.; Oppermann, U.; Schreiber, S. L.; Wang, X. A selective inhibitor and probe of the cellular functions of Jumonji C domain-containing histone demethylases. *J. Am. Chem. Soc.* **2011**, *133*, 9451–9456.

(16) Hamada, S.; Suzuki, T.; Mino, K.; Koseki, K.; Oehme, F.; Flamme, I.; Ozasa, H.; Itoh, Y.; Ogasawara, D.; Komaarashi, H.; Kato, A.; Tsumoto, H.; Nakagawa, H.; Hasegawa, M.; Sasaki, R.; Mizukami, T.; Miyata, N. Design, synthesis, enzyme-inhibitory activity, and effect on human cancer cells of a novel series of Jumonji domain-containing protein 2 histone demethylase inhibitors. *J. Med. Chem.* **2010**, *53*, 5629–5638.

(17) Sekirnik, R.; Rose, N. R.; Thalhammer, A.; Seden, P. T.; Mecnović, J.; Schofield, C. J. Inhibition of the histone lysine demethylase JMJD2A by ejection of structural Zn(II). *Chem. Commun.* **2009**, 6376–6378.

(18) Rai, G.; Kawamura, A.; Tumber, A.; Liang, Y.; Vogel, J. L.; Arbuckle, J. H.; Rose, N. R.; Dexheimer, T. S.; Foley, T. L.; King, O. N.; Quinn, A.; Mott, B. T.; Schofield, C. J.; Oppermann, U.; Jadhav, A.; Simeonov, A.; Kristie, T. M.; Maloney, D. J. Discovery of ML324, a JMJD2 demethylase inhibitor with demonstrated antiviral activity. *Probe Reports from the NIH Molecular Libraries Program*; National Center for Biotechnology Information (US): Bethesda, MD, 2010–2012.

(19) Kruidenier, L.; Chung, C. W.; Cheng, Z.; Liddle, J.; Che, K.; Joberty, G.; Bantscheff, M.; Bountra, C.; Bridges, A.; Diallo, H.; Eberhard, D.; Hutchinson, S.; Jones, E.; Katso, R.; Leveridge, M.; Mander, P. K.; Mosley, J.; Ramirez-Molina, C.; Rowland, P.; Schofield, C. J.; Sheppard, R. J.; Smith, J. E.; Swales, C.; Tanner, R.; Thomas, P.; Tumber, A.; Drewes, G.; Oppermann, U.; Patel, D. J.; Lee, K.; Wilson, D. M. A selective jumonji H3K27 demethylase inhibitor modulates the proinflammatory macrophage response. *Nature* **2012**, *488*, 404–408.

(20) Hutchinson, S. E.; Leveridge, M. V.; Heathcote, M.; Francis, P.; Williams, L.; Gee, M.; Munoz-Muriedas, J.; Leavens, B.; Shillings, A.; Jones, E.; Homes, P.; Baddeley, S.; Chung, C. W.; Bridges, A.; Argyrou, A. Enabling lead discovery for histone lysine demethylases by

high-throughput RapidFire mass spectrometry. *J. Biomol. Screening* **2012**, *17*, 39–48.

(21) Wong, B. W.; Kuchnio, A.; Bruning, U.; Carmeliet, P. Emerging novel functions of oxygen-sensing prolyl hydroxylase domain enzymes. *Trends Biochem. Sci.* **2013**, *38*, 3–11.

(22) pIC₅₀ data reported are the mean of at least two values with SEM ≤ 0.3 in all cases with the following exceptions: KDM4A RFMS, *n* = 1 for **44**, **45**; KDM6B RFMS, *n* = 1 for **24**.

(23) Diaz, R.; Luengo-Arratta, S. A.; Seixas, J. D.; Amata, E.; Devine, W.; Cordon-Obras, C.; Rojas-Barros, D. I.; Jimenez, E.; Ortega, F.; Crouch, S. Identification and characterization of hundreds of potent and selective inhibitors of *Trypanosoma brucei* growth from a kinase-targeted library screening campaign. *PLoS Neglected Trop. Dis.* **2014**, *8*, e3253.

(24) Compounds **12–15**, **17–34**, **36–39**, and **41–43** have been disclosed in the following patent application: Barker, M. D.; Campbell, M.; Diallo, H.; Douault, C.; Humphreys, P.; Liddle, J.; Sheppard, R. J.; Thomas, P. J.; Wilson, D. M. Demethylase enzymes inhibitors. PCT Int. Appl. WO2013143597, 2013. Compound **37** has also been disclosed in the following patent application: Chen, Y. K.; Kanouni, T.; Nie, Z.; Stafford, J. A.; Veal, J. M.; Wallace, M. B. Histone demethylase inhibitors. PCT Int. Appl. WO2014100818, 2014.

(25) Joberty, G.; Boesche, M.; Brown, J. A.; Eberhard, D.; Garton, N. S.; Muelbaier, M.; Ramsden, N.; Reader, V.; Rueger, A.; Sheppard, R. J.; Westaway, S. M.; Bantscheff, M.; Lee, K.; Wilson, D. M.; Prinjha, R. K.; Drewes, G. Interrogating the druggability of the 2-oxoglutarate-dependent dioxygenase target class by chemical proteomics. Unpublished results, 2015.

(26) Westaway, S. M.; Preston, A. G. S.; Barker, M. D.; Brown, F.; Brown, J. A.; Campbell, M.; Chung, C.-W.; Drewes, G.; Eagle, R.; Garton, N.; Gordon, L.; Haslam, C.; Hayhow, T. G.; Humphreys, P. G.; Joberty, G.; Katso, R.; Kruidenier, L.; Leveridge, M.; Pemberton, M.; Rioja, I.; Seal, G. A.; Shipley, T.; Singh, O.; Suckling, C. J.; Taylor, J.; Thomas, P.; Wilson, D. M.; Lee, K.; Prinjha, R. K. Cell penetrant inhibitors of the KDM4 and KDM5 families of histone lysine demethylases. 2. Pyrido[3,4-*d*]pyrimidin-4(3*H*)-one derivatives. *J. Med. Chem.* **2016**, *10.1021/acs.jmedchem.5b01538*.